



Cite this: DOI: 10.1039/d5su00583c

Received 12th July 2025  
Accepted 28th October 2025

DOI: 10.1039/d5su00583c  
[rsc.li/rscsus](http://rsc.li/rscsus)

## Carbon dots in agriculture: fundamentals, applications and perspectives

Wenna Huang, Xiaotong Zhao, Yifan Zhang, Qiluan Cheng,\* Zuojun Tan \* and Hongwei Lei 

Carbon dots (CDs) have garnered significant attention since their discovery in 2004. Their excellent optoelectronic properties, superior biocompatibility, and ecological friendliness make them very promising for sustainable agricultural applications. In this review, the synthesis strategies of CDs are first summarized and the photoluminescence mechanisms, with a specific focus on linking these fundamentals to their functions in agricultural production, are elucidated. Then the diverse applications of CDs in agriculture are detailed, specifically highlighting their roles as photosynthetic efficiency enhancers, light-conversion films and LEDs for controlled-environment agriculture, and versatile nanosensors for detecting critical agricultural metrics. Finally, the current challenges and prospects of CDs are discussed to guide their further innovative exploration in agriculture.

### Sustainability spotlight

Carbon dots (CDs) have emerged as a promising nanomaterial since 2004 due to their unique properties, including photoluminescence, biocompatibility, and eco-friendliness. These attributes make them highly relevant for sustainable agricultural applications. Developing cost-effective and scalable synthesis methods, elucidating their photoluminescence mechanism, and exploring their agricultural potential are crucial for future sustainable development. Reviewing the recent advancements in CDs can help promote green transformation, and advance efficient and sustainable development of agriculture. This work aligns well with United Nations Sustainable Development Goal 12 (Ensuring sustainable consumption and production patterns) and Sustainable Development Goal 2 (Ending hunger, achieving food security and improved nutrition, and promoting sustainable agriculture).

## 1. Introduction

Carbon-based nanomaterials are an important class of materials primarily composed of carbon atoms at the nanoscale and exhibiting diverse structures. Since their first discovery in 2004,<sup>1</sup> these materials have attracted widespread attention from researchers due to their high surface area, unique electronic structure, and tunable properties. Among these carbon-based nanomaterials, carbon dots (CDs) stand out because of their zero dimensionality, strong fluorescence, and high biocompatibility. CDs have recently emerged as a powerful, environmentally benign nanotechnology driving sustainable agriculture. Typically, CDs are defined as small nanoparticles with dimensions less than 10 nm.<sup>2</sup> Based on the different structures and properties, CDs are classified into four categories: graphene quantum dots (GQDs), carbon quantum dots (CQDs), carbon nanodots (CNDs), and carbonized polymer dots (CPDs) (Fig. 1).<sup>3,4</sup> GQDs consist of single-layer graphene or a few atomic layers, with functional groups on the edge of their carbon core. CQDs typically possess a spherical or quasi-spherical morphology with a crystalline carbon core

(comprising a hybrid of  $sp^2$  and  $sp^3$  carbon), which is different from the extended planar structure of GQDs. CNDs, in contrast, are defined by their predominantly amorphous and disordered carbon core, which distinguishes them from the crystalline nature of CQDs and the planar lattice of GQDs. The carbon core of CPDs can be further divided into several subclasses: a complete carbonization core similar to CQDs and CNDs,

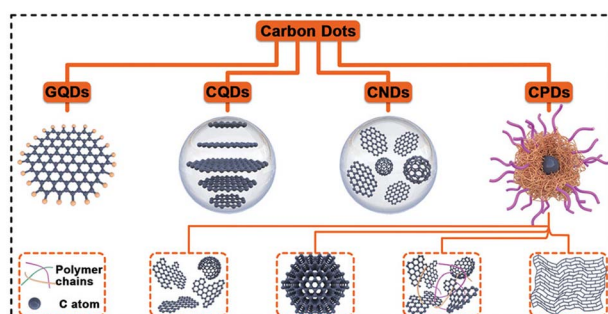


Fig. 1 Four categories of carbon dots and their structures: graphene quantum dots (GQDs), carbon quantum dots (CQDs), carbon nanodots (CNDs), and carbonized polymer dots (CPDs). Reproduced from ref. 4 with permission from Wiley, copyright 2021.



a paracrystalline carbon structure composed of tiny carbon clusters surrounded by polymer frames, and a highly dehydrated crosslinking and close-knit polymer frame structure.<sup>5</sup> The diversity of CDs is largely attributed to the differences in carbon sources and synthesis methods.

The precursors of CDs encompass a broad spectrum of materials, primarily including organic compounds and inorganic substances. The methodologies for synthesizing CDs can be broadly categorized into two primary approaches: the top-down method and the bottom-up method. The top-down method usually strips CDs from bulk carbon materials such as graphite,<sup>6–8</sup> graphene,<sup>9–11</sup> carbon nanotubes,<sup>12,13</sup> carbon fibers,<sup>14,15</sup> etc. In contrast, the bottom-up method synthesizes CDs using carbon-containing small molecules such as glucose,<sup>16–18</sup> sucrose,<sup>19,20</sup> and citric acid.<sup>21,22</sup> The choice of these methods often depends on the desired properties of the CDs and their intended application. Considerable efforts have been devoted to developing easy, cost-effective, and large-scale preparation methods. Recently, researchers reported the green synthesis of CDs by hydrothermal methods at atmospheric pressure. By heating rice husks at 220 °C with a solid loading of 3% w/v, CDs with high quantum yields can be synthesized rapidly and on a large scale.<sup>23</sup> Despite the significant advancements in the synthesis and preparation of CDs, their luminescence mechanism remains under debate. Currently, the main views on the PL origin of CDs can be summarized as the surface state, the carbon core state, and the molecular state.<sup>24</sup> The luminescence wavelengths of CDs can be modulated from ultraviolet to near-infrared by controlling size distributions and surface states, making CDs useful as biomarkers,<sup>25</sup> imaging,<sup>26</sup> lighting sources, sensors, and other optoelectronic devices for agriculture.<sup>27,28</sup>

CDs are emerging as a powerful, multi-functional tool poised to revolutionize sustainable and precision agriculture. Their exceptional optical properties enable the crucial function of improving photosynthetic efficiency, optimizing the spectral output of LEDs and light conversion films for use in controlled-environment agriculture. Furthermore, the high fluorescence and versatile surface chemistry of CDs are key to developing highly sensitive nanosensors capable of real-time detection and quantification of critical agricultural metrics, including heavy metals, antibiotic residues, and plant hormones. Besides, their biocompatibility allows for *in vivo* sensing and imaging within living plants. These applications of CDs in sustainable agriculture help meet the global food demand while maintaining environmental resilience. However, the synthesis methods, fluorescence mechanism, and applications of CDs in agricultural production are not comprehensively understood. This review aims to summarize the fundamental understanding and the applications of CDs in the field of agriculture, to provide theoretical support and practical guidance for the innovation of agricultural science and technology, and to further promote the green transformation and efficient development of agriculture.

## 2. Synthesis of CDs

In the past decade, scientists have made significant efforts to develop facile, high-yield, cost-effective, eco-friendly, and large-scale methods for the preparation of CDs. In principle, the synthetic methods of CDs can be mainly divided into two categories: top-down and bottom-up, based on the difference in carbon source (Fig. 2).<sup>29</sup> By using the top-down method, CDs were achieved by breaking down bulk materials, such as graphite,<sup>30</sup> graphene,<sup>31</sup> carbon rods,<sup>32</sup> carbon nanotubes,<sup>33</sup> and

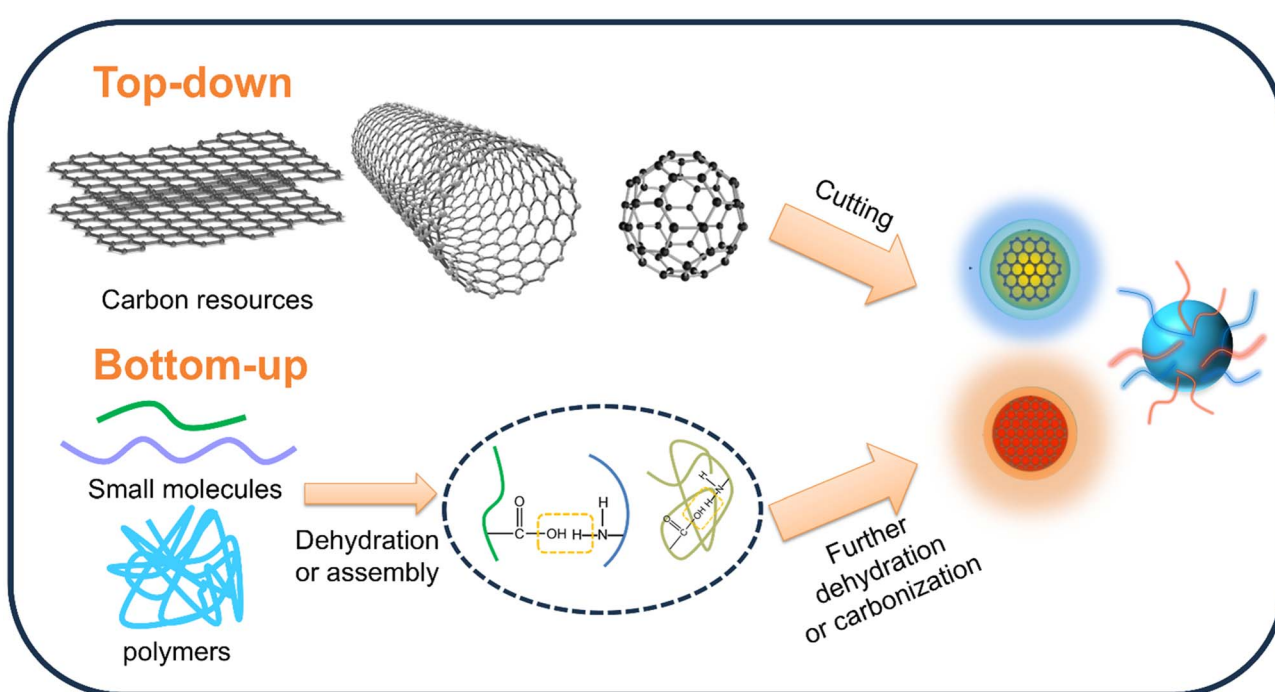


Fig. 2 Schematic illustration of two classical synthesis routes for CDs: the top-down method and the bottom-up method.



Table 1 Research progress on the synthesis of CDs

	Synthesis	Precursor	Size [nm]	Ex/Em [nm]	Quantum yield	Characterization method	Ref.
Top-down	Ultrasonic-assisted liquid phase exfoliation technique	Acetylene black	2–6	310–490/ 428–528	—	XRD, AFM, FT-IR, XPS, UV-Vis	48
	Chemical oxidation method	Graphite	2–2.8	460/540	—	UV-Vis absorption, fluorescence spectroscopy	30
	Electrochemical method	Coke	2.44–3.36	340/440	19.27%	UV-Vis absorption, fluorescence spectroscopy, SEM-EDS	41
		Carbon rods	5	—	—	Confocal microscopy, synchrotron radiation X-ray fluorescence	32
Bottom-up	Laser-ablation method	MWCNTs	1–5	360/430	12%	HR-TEM, XPS, UV-Vis absorption, fluorescence spectroscopy	45
	Hydrothermal method	CA	3.4–4.5	320–400/ 430–480	52.6%	UV-Vis absorption, fluorescence spectroscopy, FT-IR, XPS	49
		Calcein	1.4–2.8	490/530	21.9%	Zeta potential analyzer, UV-Vis absorption, fluorescence spectroscopy, STEM, XRD	50
		CA, <i>o</i> -PDA	2.2–3.8	370/440	92.1%	TEM, UV-Vis absorption, fluorescence spectroscopy, XPS, FT-IR, XRD	51
		<i>o</i> -PDA	1.8–3.7	—	25.4%	TEM, zeta potential analyzer, UV-Vis absorption, fluorescence spectroscopy, FT-IR	52
		<i>Gardenia</i> fruit Pseudo-stem of banana plant	1.2–3.5 2–3	360/450 340/460	10.7% 48%	TEM, XPS, FT-IR, XRD	53
		Corn stalk shell	1.2–3.2	365/460	16%	UV-Vis absorption, fluorescence spectroscopy, FT-IR, XPS, Raman spectrum	54
						TEM, XRD, FT-IR, UV-Vis absorption, fluorescence spectroscopy	55
	Small-molecule- precursor pyrolysis method	CA	1.4–3.3	340/425	19.2%	TEM, XPS, FT-IR, UV-Vis absorption, fluorescence spectroscopy, zeta potential analyzer	56
	Microwave-assisted method	CA	1–5	350/430	10.7%	Fluorescence spectroscopy, UV-Vis absorption, TEM, EDX	57
		Resorcinol, OPD	4.9–7.3	398/555	62.8%	Fluorescence spectroscopy, TEM, FT-IR, XRD, XPS	58
	Solvothermal method	Lychee waste	1.4–4.3	365/443	23.5%	Fluorescence spectroscopy, UV-Vis absorption, TEM, XRD, XPS	59

other indispensable materials into the nano-scale. In contrast, the bottom-up approach was based on the carbonization and polymerization of small organic molecules and polymers. Table 1 summarizes different synthetic methods along with their sizes, quantum yields, *etc*. Note that the synthesis method would critically influence the properties of CDs and impose limitations on their agricultural applications. Top-down approaches, while benefiting from inexpensive and readily available carbon sources,<sup>34</sup> typically require strong acids or

oxidants, increasing their environmental burden.<sup>35</sup> Conversely, bottom-up methods offer milder reaction conditions and facile functionalization but suffer from precursor-dependent outcomes, batch-to-batch variation, and complex reactions that hinder precise control over the final CD properties.<sup>36,37</sup> This contradiction highlights the lack of standardized and scalable synthetic schemes, which calls for further in-depth research and optimization by researchers to enhance the repeatability and reliability of CDs in agricultural applications.



## 2.1 Top-down methods

Chemical oxidation methods, among the earliest approaches for the synthesis of CDs, typically employ strong acids with oxidizing properties, such as  $\text{HNO}_3$  and the mixture of  $\text{H}_2\text{SO}_4$  and  $\text{HNO}_3$ , to oxidatively cut bulk carbon sources into CDs. This method introduces abundant oxygen-containing functional groups on the surface of CDs, endowing them with excellent dispersibility in water. Liu *et al.* used readily available and inexpensive candle soot, refluxed with  $\text{HNO}_3$ , to synthesize multicolor CDs, which presented great potential in fluorescence labels *in vitro* and *in vivo*. Their work motivated the curiosity of researchers to explore the exact chemical identities and fluorescence mechanisms of CDs and has attracted continuous attention until now. However, the use of strong acid as an oxidant requires time-consuming post-treatment, including purification (e.g., dialysis, filtration) and neutralization of excess acid, which results in irreversible environmental damage.<sup>38</sup> To avoid this problem, Zhou *et al.* demonstrated that CDs can be directly produced by oxidizing and cutting graphene oxide (GO) into nanoscale without any further purification and by-products. In their method, hydroxyl radicals ( $\cdot\text{OH}$ ), which were generated from the decomposition of  $\text{H}_2\text{O}_2$  with catalytic tungsten oxide ( $\text{W}_{18}\text{O}_{49}$ ) nanowires, were used as oxidants to synthesize CDs. The underlying mechanism of CD formation involves the selective attack of hydroxyl radicals ( $\cdot\text{OH}$ ) on the carbon atoms that are part of the GO lattice and bonded to oxygen-containing functional groups (such as hydroxyl and epoxide). This preferential oxidation weakens the adjacent C–C or C=C bonds, ultimately leading to the cleavage of the GO sheets into small CDs.<sup>39</sup> Thus, the size of CDs can be accurately controlled by adjusting the concentration of  $\cdot\text{OH}$ .

Electrochemical methods normally use bulk carbon material with good electroconductivity as a working electrode and carbon source. During the electrochemical cycle, guest ions or free radicals act as electrochemical scissors, exfoliating CDs from the working electrode. The electrochemical method of directly synthesizing CDs was first proposed by Ding's group. They employed a three-electrode system, including a working electrode made of multiwalled carbon nanotubes (MWCNTs) grown on carbon paper, a degassed acetonitrile solution with 0.1 M tetrabutylammonium perchlorate (TBAP) as the supporting electrolyte, Pt wire as the counter electrode, and an  $\text{Ag}/\text{AgClO}_4$  reference electrode.<sup>40</sup> TBA cations intercalated into the gaps during electrochemical cycling and broke the tubes near the defects. Then, CDs were exfoliated from MWCNTs. Inspired by this work, Wang *et al.* developed a one-step electrochemical exfoliation method to synthesize CDs using a two-electrode system. This system contained  $(\text{NH}_4)_2\text{S}_2\text{O}_8$  electrolyte dissolved in a mixture of MeOH and  $\text{H}_2\text{O}$  with different volume ratios. As shown in Fig. 3a, the lump coke served as the working electrode, and a platinum plate electrode acted as the counter electrode. This method provided an effective way to accurately modulate the emission position of CDs by adjusting the applied current density and water content in the electrolyte. The mechanism of exfoliated CDs from coke included two steps: (1)  $\cdot\text{OH}$  and  $\cdot\text{O}$  steamed from water decomposition peeled off coke

into a multilayer graphene sheet, and assaulted the edge sheet followed by hydroxylation or oxidation of the edge, which made the edge planes to unfold the more edge sheets; (2)  $\text{SO}_4^{2-}$  radicals facilely intercalated into sheets and split the sheet to generate CDs with a good crystalline state.<sup>41</sup> Despite this, electrochemical methods face problems such as diverse electrode materials, complex electrolyte compositions, and various potential window selections, which make it difficult to uniformly verify the yield, size, and photoelectric properties of CDs in different studies. For instance, Zhang *et al.* prepared boron-doped CDs by electrochemical exfoliation of boron-doped graphene rods.<sup>42</sup> Another study employed carbon-free electrodes to prepare CDs through a one-pot electrochemical carbonization.<sup>43</sup> Although these methods have expanded the diversity of electrochemical synthesis, the introduction of more variables due to factors such as electrode modification and electrolyte formulation has further exacerbated the reproducibility challenge.

Laser-ablation methods generally adopt high-energy laser pulses to bombard carbon-based targets to obtain carbon nanoparticles, which are subsequently passivated with polymer to improve the photoluminescence quantum yield (PLQY). The PL emission of the CDs can be tailored by laser wavelength and the input of laser fluence. Sun *et al.* first obtained multicolor CDs by using an Nd:YAG laser to ablate the mixture of graphite powder and cement in the presence of water vapor with argon as the carrier gas at 900 °C and 75 kPa. Although this approach offered a novel way to prepare CDs, the harsh synthesis conditions and complex post-processing, such as necessary passivation treatment, limited its practical application.<sup>44</sup> To simplify the synthesis process, Kang *et al.* used one-step pulsed laser ablation to peel MWCNTs from dispersed organic solvents (*n*-hexane or ethanol) to obtain CDs. CDs were rapidly obtained with homogeneous shape and size in 6 min without any passivation. The solvents utilized in the synthesis could adjust the fluorescence property of CDs (Fig. 3b).<sup>45</sup> The thin walls of MWCNTs minimized the thermal interaction between the laser and precursor *via* a photolytic process, which can lead to homogeneous size distribution of the exfoliated QDs. Overall, the laser-ablation method has high requirements for equipment, consumes a lot of energy, and the quality of the synthesis is difficult to control. This significantly increases the complexity and cost of the process, making it difficult to achieve large-scale production and application. On this basis, low-cost and high-quality synthetic methods need to be further explored.

## 2.2 Bottom-up methods

Hydrothermal methods, involving polymerization and carbonization precursors under comparatively high temperature and pressure in a Teflon-lined autoclave, are widely adopted to generate CDs.<sup>46</sup> In 2010, Zhang *et al.* first used the small organic molecule L-ascorbic acid as the carbon source, and a mixture of  $\text{H}_2\text{O}$  and ethanol as the solvent, to directly synthesize mono-disperse water-soluble CDs with an emission peak at 420 nm *via* a hydrothermal reaction.<sup>47</sup> The low PLQY (6.76%) and monotonous fluorescence limited their potential for practical



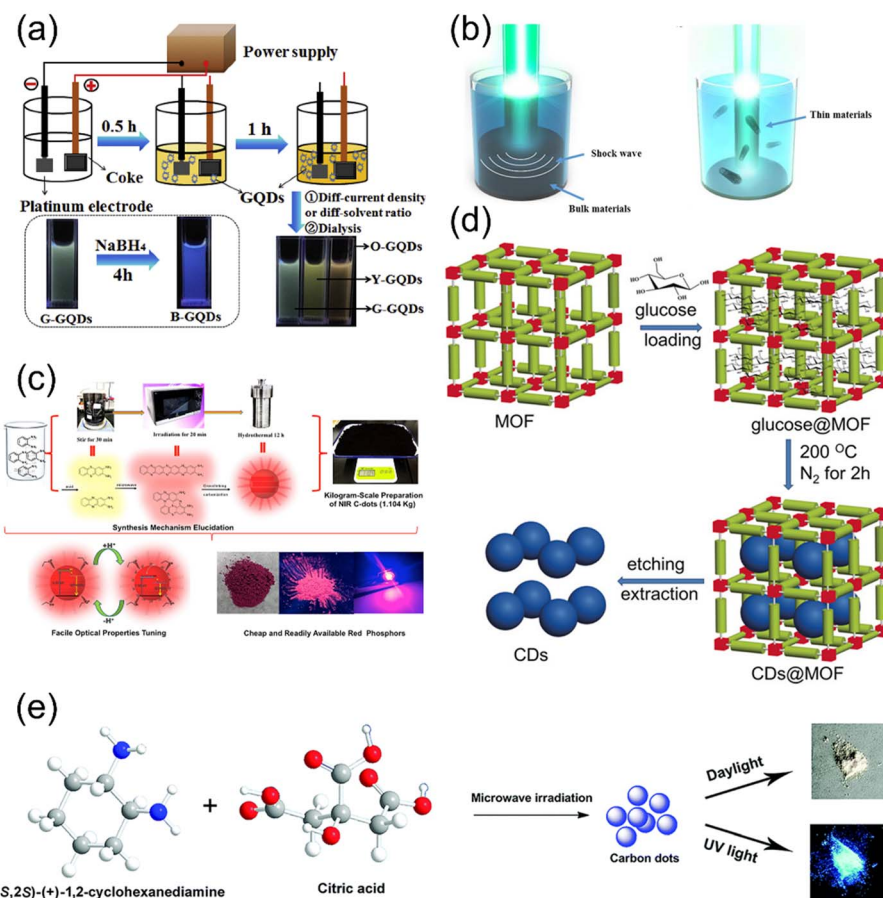


**Fig. 3** (a) Schematic illustration of the synthetic process of multicolor GQDs from coke. Reproduced from ref. 41 with permission from Elsevier, copyright 2018. (b) Schematic diagram of the pulsed laser ablation process. Reproduced from ref. 45 with permission from Nature, copyright 2016. (c) Schematic illustration showing the synthesis process of C-dots on a kilogram-scale. Reproduced from ref. 52 with permission from Elsevier, copyright 2022. (d) Schematic diagram of photoluminescent carbon nanodots prepared using porous MOF templates. Reproduced from ref. 63 with permission from Wiley Online Library, copyright 2017. (e) The synthesis of SSF-emitting CD powder. Reproduced from ref. 65 with permission from RSC, copyright 2021.

application. Inspired by their findings, Miao *et al.* prepared multicolor N-doped CDs with blue-, green-, and red-emission (B-CDs, G-CDs, R-CDs) by adjusting the ratios of citric acid to urea and the temperature of the solvothermal reaction. They demonstrated that the maximum emission of the CDs shifted from blue to red as the temperature and molar ratio increased. This shift was attributed to the increased conjugation length and surface functional groups such as carboxyl ( $-\text{COOH}$ ).<sup>49</sup> Zhu *et al.* used calcein as a fluorescent precursor to prepare CDs with triple-emission of UV, blue, and green. These emissions were attributed to the original pyrolysis product of ethanol in NaOH, surface defects, and calcein chromophore on the surface of the CDs. Mixing CDs with rhodamine B (RhB) can create a CDs/RhB composite with triple-emission in the visible region, functioning as a multicolor sensor in cell imaging.<sup>50</sup> CDs with ultra-high PLQY of 92.1% and excellent dispersibility were hydrothermally synthesized using CA and *o*-phenylenediamine (*o*-PDA) as carbon and nitrogen sources, respectively.<sup>51</sup>

Despite these advancements, the absence of large-scale and high-yield preparation methods is still considered an obstacle limiting their application. To address this, Ji *et al.* developed

a kilogram-scale preparation of near-infrared CDs (NIR-CDs) with a cost of only 0.1\$ per gram and a yield exceeding 96%. They used *o*-phenylenediamine (*o*-PDA) dissolved in an aqueous solution of sulfuric acid mixed with 3-chloroperbenzoic acid, followed by treatment with microwave radiation and hydrothermal reaction (Fig. 3c).<sup>52</sup> Under microwave radiation and with the oxidization agents, the polymerization of the dimer 2,3-diaminophenazine (DAP) was initiated. DAP is formed from the self-condensation of two molecules of *o*-PDA in an acidic environment. Then, the energy provided by the hydrothermal reaction further polymerized and carbonized these larger molecules to generate CDs with an emission peak located at 653 nm. These CDs were sensitive to pH changes, resulting in the emission peak rapidly shifting from blue to 606 nm with an increase in PLQY from 8.2% to 25.4% after alkali treatment. However, subtle changes in reaction parameters of hydrothermal/solvothermal methods (such as temperature, time, precursor ratio, pH value, *etc.*) can significantly affect the growth process of CDs, influencing the predictability of material design and reproducibility of the synthesis.

Another popular bottom-up strategy to synthesize CDs is the small-molecule-precursor pyrolysis method, in which CDs can be obtained from precursors that undergo decomposition and carbonization at high temperatures. Inspired by the hot injection method, a traditional approach for preparing semiconductor quantum dots and nanocrystals, Wang *et al.* synthesized CDs by pyrolyzing CA in the hot noncoordinating solvent octadecene (ODE) mixed with 1-hexadecylamine (HDA) or polyethylene glycol (PEG<sub>1500N</sub>) at 300 °C. They found that the emissive peak and hydrophilicity/hydrophobicity of CDs can be simplistically adjusted by manipulating the reaction time and surface passivation agent, respectively.<sup>60</sup> Furthermore, CDs were generated directly through the pyrolysis of a solvent-free precursor solution. J. Krysmann *et al.* employed a mixture of CA and ethanolamine (EA) at a molar ratio of 1:3, which was refluxed in air at different temperatures, to systematically investigate the formation mechanism of CDs.<sup>61</sup> Molecular fluorophores with high PLQY were formed at low temperatures. As the temperature increased, the formation of the carbogenic core ensued, accompanied by the loss of molecular fluorophores. Eventually, the PL may predominantly and even exclusively arise from the carbogenic core at high temperatures. In other cases, Rong *et al.* developed a one-pot solid-phase pyrolysis method, which involved directly heating guanidinium chloride and CA in a round-bottom flask at 225 °C to prepare N-doped CDs with a PLQY of 19.2%. These CDs exhibited good stability and functioned as fluorescence probes to detect the Fe<sup>3+</sup> in aqueous solution.<sup>56</sup> Furthermore, it is worth noting that immobilizing the precursor into a suitable template, such as porous materials, has been recognized as an effective approach to inhibit the aggregation of products and the generation of by-products during the pyrolysis process for obtaining homogeneous CDs.<sup>62</sup> Gu *et al.* calcined and carbonized the glucose loaded into the pores of well-defined metal-organic frameworks (MOFs) at 200 °C in a nitrogen atmosphere for 2 h. Then they produced an array of uniform CDs that contained the intact MOFs. In addition, the size of resulting CDs can be precisely tuned by adjusting the pore sizes of MOFs (Fig. 3d).<sup>63</sup>

Hydrothermal/solvothermal and small-molecule-precursor pyrolysis methods are recognized as optimal strategies for the synthesis of CDs due to their facile manipulation and functionalization. However, these methods suffer from time and energy-consuming issues. To avoid these problems, microwave-assisted methods have been introduced as a facile, rapid, and economic strategy for synthesizing CDs. Unlike conventional heating methods, in which the energy is delivered to the surface of the material *via* radiant and/or convection heating and transferred to the material's bulk *via* conduction, the energy of microwave-assisted methods absorbed by carbon material is transformed by dielectric heating. This process provides homogeneous and fast heating, resulting in fast preparation of high-quality CDs.<sup>64</sup> Samah *et al.* prepared blue-fluorescence nitrogen/sulfur co-doped carbon dots (N, S-CDs) with narrow size distribution and good hydrophilicity using microwave-assisted pyrolysis of CA and thiosemicarbazide in a microwave oven within 60 s. The production yield was about 64.38 wt%. Because the fluorescence of CDs was merely quenched by Cu<sup>2+</sup>

and restored by complexation of Cu<sup>2+</sup> with etidronate disodium (ETD),<sup>57</sup> these CDs were validated as selective and rapid turn-off-on fluorescent probes for both copper (Cu<sup>2+</sup>) and ETD. Yang *et al.* synthesized yellow-emitting CDs with a PLQY of 62.8% by using resorcinol and *o*-phenylenediamine as precursors under microwave radiation heated at 180 °C. CDs were incorporated into polyvinyl alcohol (PVA) to form the CDs/PVA film, which presented excellent water-induced shape recovery behavior and responsiveness tuned by changing the environment.<sup>58</sup> Moreover, Wang *et al.* successfully prepared self-quenching-resistant solid-state fluorescence-emitting CDs with a high absolute PLQY of 51.7% *via* the one-step microwave-assisted method using citric acid as the carbon source and cyclohexanediamine as the passivant. The cyclohexanediamine can introduce steric hindrance to the surface of the CDs, thus weakening the π-π interaction in a state of aggregation and overcoming the aggregation-induced fluorescence quenching (Fig. 3e).<sup>65</sup> Besides, natural renewable sources have also been selected as a carbon source to synthesize CDs.<sup>66</sup> Plant-derived biomass, animal-derived biomass, and even waste like food/kitchen waste, agricultural residues, and municipal solid waste have been confirmed as ideal raw materials for the synthesis of CDs.<sup>67</sup>

### 3. Fluorescence mechanism of CDs

CDs display excellent fluorescence emission properties. Elucidating the PL mechanism of CDs is crucial for precisely regulating their optical properties, realizing their applications in various fields, especially in agriculture. PL has two basic forms: fluorescence and phosphorescence, and its underlying mechanism can be clearly described using a Jablonski diagram. Investigations into the CDs' PL mechanism have indicated that PL results from the interplay of multiple factors. Researchers identified three fluorescence mechanisms: size-dependent emission (determined by the carbon core),<sup>68</sup> surface defect state emission (determined by the carbon backbone and attached chemical groups),<sup>69-72</sup> and molecular state emission (determined by fluorescent molecules on the surface or interior of CDs).<sup>73</sup> Different interpretations of the photoluminescence properties of CDs are likely due to differences in the raw materials or precursors, or different synthesis strategies. A comprehensive understanding of the individual contributions from the carbon core size, surface functional groups, and molecular fluorophores can be achieved through systematic analysis of excitation-dependent emission behavior, fluorescence lifetime decay, and post-synthesis treatments such as chemical etching and surface passivation. Correlating these findings with spectroscopic data from Raman, XPS, and FTIR techniques provides further mechanistic insights (Table 1), thereby effectively bridging fundamental mechanistic studies with practical agricultural application requirements.

#### 3.1 Carbon core state

Carbon core state, also known as the quantum confinement effect or size effect, refers to fluorescence resulting from π-π\*

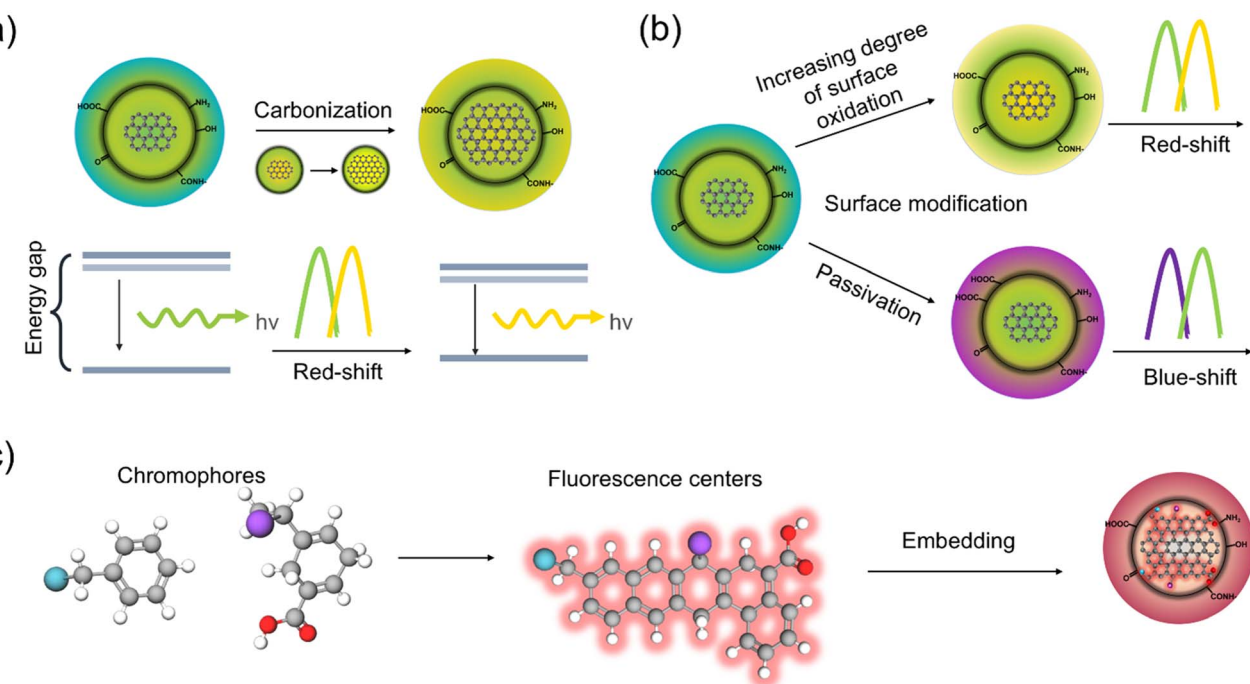


Fig. 4 (a) Carbon core state luminescence. (b) Surface state luminescence. (c) Molecular state luminescence.

electron transition at a higher energy level. The “size” in “size effect” is the isolated  $sp^2$  (graphene) subdomain, known as the effective conjugation length, rather than the actual size of CDs.<sup>74</sup> For CDs, if the conjugated  $sp^2$  domain size decreases, the electron’s confinement is heightened, resulting in a widened energy bandgap. Consequently, the CDs would emit higher-energy, shorter-wavelength light, thus establishing a direct, size-dependent tuning of the emission color. This model is suitable to explain the PL of GQDs,  $g$ -CNQDs, and CQDs that possess well-defined crystalline structures and a high degree of graphitization (Fig. 4a). Li *et al.* adopted an electrolysis graphite rod in an alkaline medium to synthesize CDs with different sizes.<sup>75</sup> Using silica-gel column chromatography to separate as-synthesized CDs with various diameters, they obtained four typical-sized CDs with the same crystalline structure. The results revealed the relationship between size and emission wavelength: small GQDs (1.2 nm) give UV light emission (about 350 nm), medium-sized CDs (1.5–3 nm) give visible light emission (400–700 nm), and large CDs (3.8 nm, center) give near-infrared emission (about 800 nm). There is no obvious change in the size-dependent PL or graphite fragment structure of CDs after being treated with hydrogen plasma to remove most of the oxygen-containing functional groups. This result confirms that the emission of CDs originates from the quantum-sized effect rather than from the carbon–oxygen surface. Nevertheless, density-functional theory (DFT) calculations revealed that the GQDs with a pure and complete  $sp^2$  carbon crystalline structure emitted fluorescence from deep UV to near-infrared as their size varies from 0.46 to 2.31 nm.<sup>76</sup> The combined theoretical and experimental analysis by Nikita V. *et al.* establishes that photoluminescence in CDs emanates

from spatially localized surface domains of partially  $sp^2$ -hybridized carbon embedded within an  $sp^3$ -hybridized amorphous matrix. These domains constitute the “carbon-core states”, whose electronic structure is governed solely by the  $sp^2$ -hybridization fraction  $\eta$ . The statistical distribution of  $\eta$  across the ensemble dictates: (1) inhomogeneous spectral broadening in both absorption and emission; (2) a pronounced Stokes shift originating from excited-state charge redistribution and concomitant lattice relaxation within individual domains; and (3) excitation-wavelength-dependent PL maxima arising from preferential excitation of sub-populations with differing  $\eta$ .<sup>77</sup> Subsequently, guided by these theoretical predictions, Wang *et al.* selected CA which contains an  $sp^3$  hybridized structure, and *o*-phenylenediamine (oPD), which contains an  $sp^2$  hybridized structure, as the precursor in the synthesis to hydrothermally prepare CDs with multicolor emission covered the whole visible spectrum. The spectral position of the CDs’ emission could be tuned by adjusting the ratio of  $sp^2$  and  $sp^3$  hybridized domains.<sup>78</sup> In detail, when  $NaBH_4$  and  $NaOH$  were added to reduce the functional group on the surface of CDs, the emission peak position remained unchanged. But the PL emission was red-shifted with an increase in the size and extent of  $sp^2$  hybridization.

### 3.2 Surface state

During the synthesis of CDs, defects such as oxygen and nitrogen-containing functional groups, as well as other heteroatoms, may inevitably arise on the surface of  $sp^2$  domains. Therefore, it is possible to modulate the emission sites of CDs by changing the surface functional groups, which in turn adjust the electron structure and energy level (Fig. 4b).



Xiong *et al.* employed silica column chromatography to separate urea and *p*-phenylethylamine, obtaining full-color CDs with excitation-independent PL emission.<sup>79</sup> Structural and chemical characterization revealed that CDs with different emission wavelengths exhibited similar distributions of particle size and graphite structure in carbon cores. However, the degree of oxidation on their surfaces varied, resulting in red-shifted emission peaks. This shift was attributed to a reduction in the energy band gap between the highest occupied molecular orbital (HOMO) and the lowest unoccupied molecular orbital (LUMO), as the content of oxygen atoms on the surface of the carbon core increased. This process ultimately determines the colors of their PL. On the other hand, doping can also cause a shift in the energy levels or band gaps of the CDs, leading to the formation of various emission centers and traps. This modification allows for the tuning of emission spectra, thereby enhancing the diversity of fluorescence emissions compared to their original state.<sup>80</sup> However, dopants usually exist only on the surface of CDs, which means that the doped CDs' emission spectrum largely depends on the competition among the optical centers, the surface traps, and the surface state.<sup>81</sup> It is well established that nitrogen doping reduces the band gaps and emission energy in CDs. Doping N in the carbon structure can produce positively charged carbon atoms, as N possesses a higher electronegativity (3.04) than C (2.55). Furthermore, N doping stabilizes the surface defects and increases the fluorescence emission of CDs.<sup>82</sup> Atchudan *et al.* reported that nitrogen-doped CDs derived from dwarf banana peel and aqueous ammonia using the hydrothermal method exhibited wavelength-dependent emission characteristics.<sup>83</sup> Their study revealed that fluorescence intensity increased as the excitation wavelength changed from 290 nm to 345 nm, followed by a decrease as the excitation wavelength changed from 345 nm to 460 nm. This phenomenon was attributed to the different energy levels of surface traps caused by the diversity of surface functionalities.

### 3.3 Molecule state

The molecular emission mechanism of CDs refers to the formation of fluorescence centers composed of organic chromophores in the process of CD synthesis. These chromophores are capable of direct fluorescence emission and are usually connected to the surface or interior of the carbon skeleton. The CDs with the molecular state as the luminous center have a strong fluorescence emission characteristic, often with a high brightness and short emission wavelength (Fig. 4c).<sup>74</sup> Research indicates that the reaction between the citric acid and amine precursor initially generates citrazinic acid and its derivatives as fluorophores. As the reaction continues, the polymerization and carbonization effects take place to utilize the fluorophores as the seeds for the growth of aromatic crystals.<sup>84</sup> Sara *et al.* prepared novel chromophore-doped CDs by hydrothermal treatment of glucose and 3-nitroaniline in the presence of high concentrations of sulfuric acid. These CDs had completely distinct pH-dependent emission colors of blue, red, and yellow, under acidic, neutral, and alkaline conditions, respectively.

They proved that chromophores in CD structures add new electronic transition pathways to modulate the HOMO–LUMO energy levels, reduce the electronic bandgap, and shift the absorption and emission spectra to longer wavelength regions.<sup>85</sup> Furthermore, CDs prepared with citric acid and urea by the microwave-assisted method also elucidated the molecular basis of the fluorescence mechanism, clarifying the chemical structure of the formed fluorescent compound.<sup>86</sup>

## 4. Application of CDs in agriculture

### 4.1 Improving photosynthesis in plants

Photosynthesis, the most fundamental biochemical process for sustaining life on Earth, maintains global carbon and oxygen cycles.<sup>87</sup> As illustrated in Fig. 5a, this process comprises light-dependent reactions and the Calvin–Benson cycle (formerly termed dark reactions). The light-dependent phase involves: (1) primary reactions converting light energy to electrical energy through photosynthetic electron transport on chloroplast thylakoid membranes, and (2) photophosphorylation generating energy carriers adenosine triphosphate (ATP) and nicotinamide adenine dinucleotide phosphate (NADPH). The Calvin–Benson cycle fixes atmospheric CO<sub>2</sub> into organic molecules *via* enzymatic reactions in the chloroplast stroma.<sup>88</sup> The potential efficiency at each step of photosynthesis indicates that, at 30.8 °C and with a CO<sub>2</sub> concentration of 380 ppm, the maximum light-to-biomass conversion efficiency is 4.6% for C<sub>3</sub> photosynthesis and 6% for C<sub>4</sub> photosynthesis.<sup>89</sup> Current studies indicate that while historical yield gains relied minimally on photosynthetic improvements, future productivity increases will require enhanced photosynthetic efficiency.<sup>90</sup> For instance, engineered metabolic pathways have boosted yields by 11–40% in tobacco and rice,<sup>91,92</sup> and gene editing of photoprotective components has increased the efficiency by 8–10%.<sup>93,94</sup> However, these biological approaches are complex, species-specific and costly. In contrast, CDs, with their small nano size, tunable fluorescence *via* synthesis parameter control, selective UV absorption, modifiable surface functional groups, and low cost, offer a promising alternative to overcome these bottlenecks.<sup>95–97</sup> They can serve as novel photosynthesis regulators, providing new pathways for green and sustainable agriculture (Table 2).

**4.1.1 Light reaction.** The light reactions commence with photon capture by chlorophyll *a/b* and carotenoid antenna complexes, where resonance energy transfer directs excitons to reaction center pheophytin molecules for charge separation.<sup>98</sup> Chlorophyll's conjugated porphyrin ring structure restricts absorption to two spectral regions: 640–660 nm (red) and 430–450 nm (blue-violet).<sup>99</sup> Expanding absorption into underutilized UV ranges or improving visible light utilization represents viable efficiency-boosting strategies. Studies demonstrate that CD–photosynthetic pigment (PP) conjugates exhibit enhanced 680–720 nm emissions (characteristic of PSI/PSII chlorophyll) under 350–400 nm excitation compared to isolated PPs, confirming that energy can be transferred from CDs to PPs.<sup>100</sup> Remarkably, *in vivo* experiments with *Nicotiana tabacum* showed 18% increased photosynthetic rates following intra-leaf



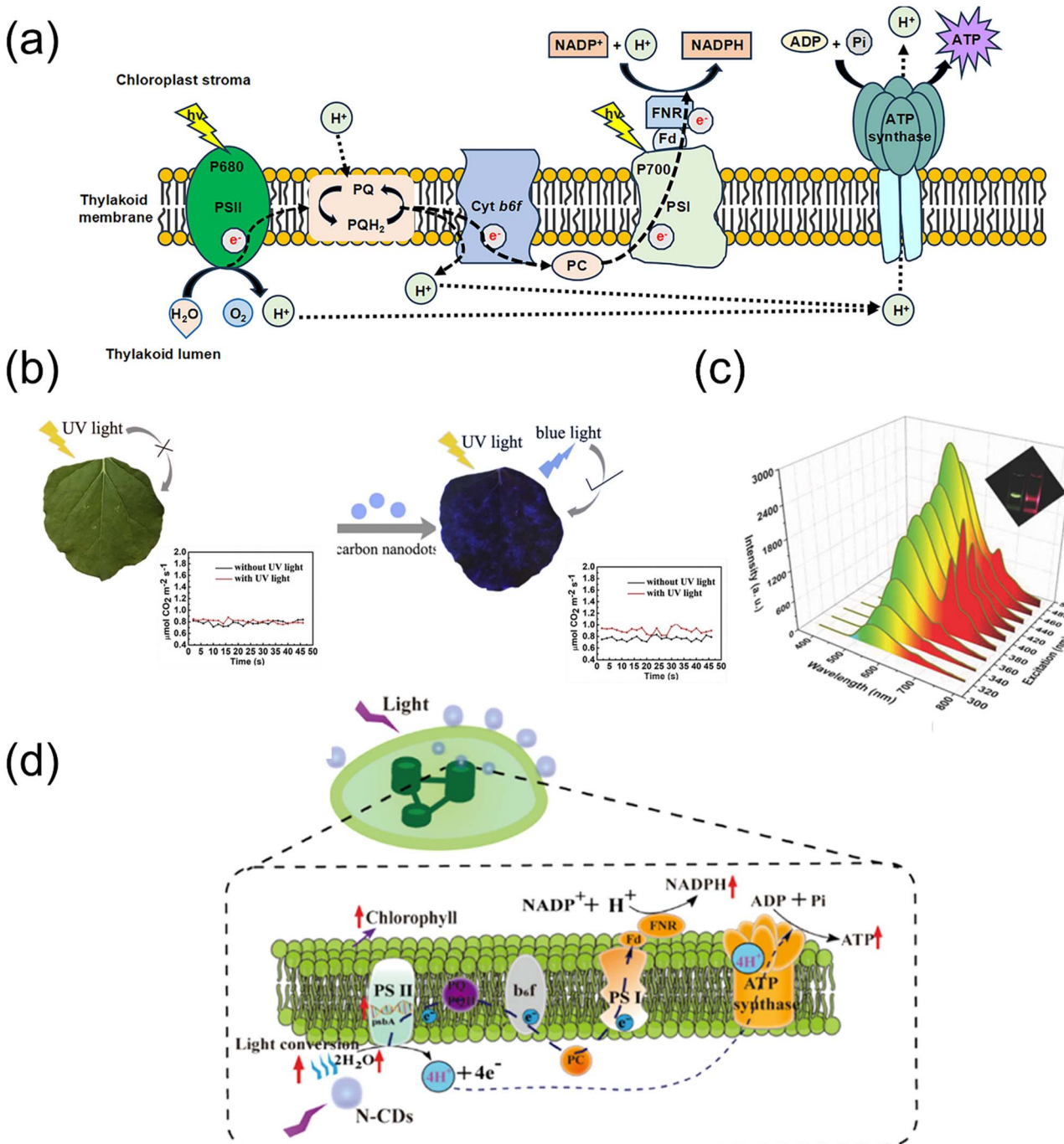


Fig. 5 (a) Schematic representation of photosynthetic light reactions and auxiliary electron transport pathways. Reproduced from ref. 88 with permission from Elsevier, copyright 2025. (b) With the help of UV-to-blue light conversion nanomaterial, the photosynthetic rate of the leaf was improved by 18%. Reproduced from ref. 101 with permission from Elsevier, copyright 2018. (c) The prepared CDs have strong fluorescence in ethanol. Reproduced from ref. 106 with permission from Elsevier, copyright 2018. (d) Photosynthetic activity enhanced by CDs and N-CDs. Reproduced from ref. 114 with permission from Wiley, copyright 2021.

injection of NH<sup>2</sup><sup>-</sup> functionalized CDs acting as UV-to-blue converters, particularly under supplemental UV illumination (Fig. 5b). To address chloroplasts' limited short-wavelength utilization, researchers developed near-infrared (NIR) and far-infrared (FIR) emitting CDs activated by UV light.<sup>101-103</sup> Note that both blue and red light play key roles in determining leaf

photosynthesis, and the plant cultivated in the monochromatic red or blue light will suffer a spectral "deficiency" syndrome, which can be reversed by a combination of blue and red light used as a light source.<sup>104,105</sup> Capitalizing on this, Li *et al.* engineered dual-emission chloroplast-matched blue/red CDs (Fig. 5c). These CDs enhanced hybrid photosystem performance

Table 2 Research progress of CDs in agriculture

Precursor	Mode of application	Exposure time	Linear range	Effect and function	Yield and sustainability assessment	Ref.
Citric acid monohydrate, urea, citric acid, boric acid	QD-PP hybrid system for the study of fluorescence energy transfer	24 h	—	Enhance chlorophyll fluorescence upon 360–420 nm excitation	Green precursors; non-toxic; highly biocompatible; low energy footprint (microwave heating for 7–12 min)	100
Glc, CA, EDA, PEI, BLG	<i>Nicotiana tabacum</i>	2 hours to 2 days	—	Enhance photosynthetic rate by 18% under additional UV irradiation	Low-cost precursor; the synthetic method is energy-efficient	101
<i>Phellodendron chinense</i> Schneid	The chloroplast surface of spinach and the roots of romaine lettuce plants	Spinach: 10 min, romaine lettuce: 3 days in CD-containing nutrient solution	0–10 $\mu\text{g mL}^{-1}$ ( <i>in vitro</i> ) and 0–9 $\mu\text{g mL}^{-1}$ ( <i>in vivo</i> )	ATP production increased by 2.8 times, electron transport rate increased by up to 25% in living lettuce leaves	Low-cost natural precursor	106
CA, melamine, ethylenediaminetetraacetic acid (EDTA)	Foliar spray	Seedling stage: 7 days of spraying, full life-cycle: sprayed for 5 days at day 50 and 70	—	The corn yield increased by 24.50%, and the 1000 grain weight increased by 15.03%	Biocompatible, chemically inert, and non-toxic, foliar application reduces environmental impact compared to soil application	114
CDs/CaAlSiN <sub>3</sub> :Eu <sup>2+</sup> -silica powder	Plant growth lighting	21-day plant	—	Good growth performance in lettuce and chrysanthemum	Non-toxic and biocompatible; good thermal stability (up to 250 °C); simple, low-cost, and energy-efficient preparation method	168
Anhydrous citric acid, formamide, <i>meso</i> -AlO <sub>X</sub>	Agricultural sunlight conversion films (for plant photosynthesis)	—	—	Conversion of UV light to blue/red light. High thermal stability (up to 800 °C)	Green precursor; non-toxic, renewable, environmentally friendly	129
Papaya seeds, H <sub>3</sub> PO <sub>4</sub> , CDs@LCAO:Eu <sup>3+</sup> NCS	Optical thermometry indoor plant growth lighting	UV stability test: 300 minutes, plant growth period: 55 days, LED operation: 16 hours per day	Temperature sensing: 300–480 K, CDs loading: 2–8 wt%	The plant height, stem thickness, leaf width and chlorophyll increased by 6.17%, 21.42%, 10.65% and 19.5% respectively	Eco-friendly; low-toxicity precursors; enhanced efficiency reduces energy consumption in lighting and agriculture	169
Dopamine hydrochloride, OPD	Agricultural sunlight conversion film	Film stability test: 3 days (under sunlight), plant growth experiment: 12 days	—	Increase fresh weight by 10.4%, dry weight by 13.9%, and chlorophyll $\alpha$ content by 7.1% in mung bean sprouts	The yield of RCDs is approximately 29%; biodegradable and environmentally friendly	133
NaYF <sub>4</sub> :Yb, Tm@NaYF <sub>4</sub> , PAA, EDA	Cover the film over the plant or chloroplast samples	<i>In vitro</i> : 5–9 minutes — under 10 mW cm <sup>-2</sup> , <i>in vivo</i> : 1 hour under natural light + UV (0.57 mW cm <sup>-2</sup> )	—	Enhanced photosynthesis by ~12% in <i>Arabidopsis thaliana</i>	The QY for the upconversion luminescence is 0.09% and that for the total luminescence is 7.3%; film-based application avoids direct incorporation into plant tissue	134



Table 2 (Contd.)

Precursor	Mode of application	Exposure time	Linear range	Effect and function	Yield and sustainability assessment	Ref.
Potato pulp, potassium KMnO <sub>4</sub> , HQ, C <sub>7</sub> H <sub>5</sub> ClOS	Aqueous solution detection of Hg <sup>2+</sup> in natural water	15 minutes for solution-phase detection, 2 hours for solid-phase detection	Fluorometric: 0.01–0.1 μM, colorimetric: 1–10 μM	Selective detection of Hg <sup>2+</sup>	The synthetic yield of HQTC is 91%; 100 mg of carbon dots is approximately 40 Indian rupees; biomass-derived CDs; components are stable for months	138
Glycine, AgNO <sub>3</sub> , NaBH <sub>4</sub>	Detection of sulfite/ bisulfite (SO <sub>3</sub> <sup>2-</sup> /HSO <sub>3</sub> <sup>-</sup> ) in agricultural products	—	20–200 μM	Highly sensitive and selective detection of SO <sub>3</sub> <sup>2-</sup> /HSO <sub>3</sub> <sup>-</sup>	Synthesis is simple; low cost; non-toxic; stable	142
<i>Sanghuangporus lonicericola</i>	Detection of tetracyclines (TCs) in aquaculture water and rat serum samples	Immediate response	OXY: 0.6–73.3 μM DOX: 0–95.2 μM TCY: 6.5–72.3 μM MNO: 10–52.6 μM	—	Green, sustainable, and environmentally friendly	144
Corn cob	Detection of melamine in dairy products (milk and milk powder)	—	H <sub>2</sub> O <sub>2</sub> : 1.67–16.67 mmol L <sup>-1</sup> , melamine: 1–20 μmol L <sup>-1</sup>	—	Low-cost, eco-friendly, green synthesis	145
CA, ascorbic acid, EDA, HCl	Biological imaging	Zebrafish: 6–72 hours, bacteria: 8 hours, plants: 2 days	—	High biocompatibility, effective fluorescence uptake in bacterial and plant cells	—	146

*in vitro* and boosted romaine lettuce photosynthesis *in vivo*.<sup>106</sup> However, the aggregation in vascular tissues often causes fluorescence quenching of CDs. To circumvent this, Xiao *et al.* prepared aggregation-induced emission carbon dots (CDs-AIE) and verified that these CDs-AIE enabled chloroplasts to harvest UV light *via* green/red emission, expanding the operational light spectrum.<sup>107,108</sup>

Electrons extracted from water are transported from the PSII donor side and PSI acceptor *via* three types of transmembrane complexes: the cytochrome *b*<sub>6</sub>*f* (cyt *b*<sub>6</sub>*f*), membrane-soluble plastoquinone (PQ) acting as a proton pump, and a copper-containing protein named plastocyanin (PC). In brief, cyt *b*<sub>6</sub>*f* takes electrons from PQ to PC and passes them to an electron acceptor soluble in the luminal space, which in turn reduces PSI, the PSI chlorophyll that gets stably oxidized after charge separation.<sup>109</sup> The ultimate electron acceptor is NADP<sup>+</sup> in the linear electron transport of plants, and the proton gradient across the thylakoid membrane of the chloroplast drives the synthesis of ATP. The manipulation of photosynthetic electron transport by CDs is possible to increase the rate of photosynthesis and stimulate plant growth.<sup>110</sup> Chandra *et al.* proposed that photosynthesis can be augmented by electrons transported

from amine-functionalized CD-donor to the chloroplast-acceptor *in vitro*.<sup>111</sup> The excess electrons originally from photons absorbed by CDs conjugated with chloroplasts were directly transferred to the whole linear photosynthetic electron transport chain. This increased the rate of oxygen evolution, NADP<sup>+</sup> reduction, and ATP formation, while accelerating the conversion of light energy. Light quantum absorption, charge separation, and electron transfer are conducted by two protein complexes embedded in thylakoid membranes: PSII and PSI. PSII, composed of a light-harvesting pigment protein complex (LHC), reaction center, and oxygen-evolving complex (OEC), is a key element in oxygenic phototrophs.<sup>112</sup> In brief, PSII absorbed and transferred the excitation energy of photons through photosynthetic pigments as well as charge separation products, enabling electron transport in the reaction center along with extracted electrons from H<sub>2</sub>O to generate O<sub>2</sub> with the aid of OEC.<sup>113</sup> Wang *et al.* synthesized nitrogen-doped CDs (N-CDs) and confirmed that N-CDs supply electrons to the decomposition of water in the PSII reaction center and accelerate the electron transfer rate in PSII, therefore enhancing the net photosynthetic rate of corn *in vivo* (Fig. 5d).<sup>114</sup> Xiao *et al.* also suggested that CD-AIE augmented the photosynthetic efficiency



of the chloroplast by accelerating the electron transport rate in the PSII.<sup>108</sup> The fundamental mechanism of the function of PSI was similar to PSII. In PSI, the electron is transferred from the primary electron donor  $P700^+$  (excited state of LHC) to a terminal electron acceptor formed by the special iron–sulfur (Fe–S) cluster located on the stroma, which ultimately donates an electron to the natural electron acceptor, ferredoxin *via* an internal cofactor.<sup>115</sup> Notably, Wang *et al.* identified selective CD binding to PSI Fe–S clusters (absent in PSII), facilitating electron tunneling through noncovalent interactions. This specificity suggests that CDs preferentially optimize late-stage photosynthetic electron transfer processes.<sup>116</sup>

In short, CDs have emerged as a promising tool for enhancing the light reactions of photosynthesis by expanding the spectral absorption range of chlorophyll and optimizing electron transport efficiency. Through their unique photoconversion properties, CDs enable plants to utilize underused UV and far-red wavelengths, transferring energy to PSI/PSII while functionalized CDs (*e.g.*, amine-modified or N-doped) directly participate in electron transfer, accelerating water splitting,  $NADP^+$  reduction, and ATP synthesis. However, the full potential of photosynthetic enhancement depends not only on light reactions but also on the subsequent dark reactions, where the ATP and NADPH generated are utilized for  $CO_2$  fixation.

**4.1.2 Dark reaction.** Plants employ three distinct pathways for  $CO_2$  fixation during photosynthesis: the Calvin cycle (C3 pathway), the C4-dicarboxylic acid pathway (C4 pathway), and crassulacean acid metabolism (CAM pathway).<sup>117</sup> Nevertheless, most of the global  $CO_2$  fixation occurs through the C3 pathway, primarily mediated by ribulose 1,5-bisphosphate carboxylase–oxygenase (rubisco).<sup>118</sup> Despite its essential function, the efficiency of rubisco is compromised by its low turnover rate and promiscuous dual reactivity, which catalyzes both the carboxylation and oxygenation of ribulose 1,5-bisphosphate (RuBP). The carboxylation reaction generates two molecules of 3-phosphoglycerate (3-PGA), while oxygenation produces molecules of 3-PGA and 2-phosphoglycolate (2-PG), the latter requiring energy-intensive salvage pathways (photorespiration) that result in net  $CO_2$  loss.<sup>119</sup> Recent advances demonstrate CDs' potential for enhancing the photosynthetic efficiency. Li *et al.* reported a one-step electrochemical synthesis of CDs at room temperature, using CDs as both working and counter electrodes and ultrapure water as the electrolyte. Using *Arabidopsis thaliana* and *Trifolium repens* L. as model systems, they demonstrated that CDs enhanced rubisco's activity, thereby accelerating carbon assimilation. The CDs were shown to undergo horseradish peroxidase-mediated degradation to yield plant hormone analogs or  $CO_2$ , which supported the carbon reaction. Additionally, CDs delivered water and essential trace elements ( $K^+$ ,  $Ca^{2+}$ ,  $Mg^{2+}$ ,  $Cu^{2+}$ ,  $Zn^{2+}$ ,  $Mn^{2+}$ ,  $Fe^{3+}$ ) through non-covalent interactions with surface oxygen-containing functional groups ( $-OH$ ,  $-COOH$ ), collectively promoting plant growth.<sup>32</sup> Complementary research by Zhang *et al.* demonstrated chirality-dependent effects using L/D-cysteine-derived CDs. At an optimal concentration, mung bean plants exhibited 20.5% (L-CDs) and 67.5% (D-CDs) increases in rubisco activity, correlating

with 18–39% carbohydrate accumulation enhancement compared to controls.<sup>120</sup>

To elucidate the molecular mechanisms underlying CD-enhanced photosynthesis, it is necessary to assess the photosynthesis-related gene expression patterns through transcriptomic analysis. Wang *et al.* suggested that the expression levels of *PsbP*, *Psi-K*, *PsbS1*, *PsbY*, *PsbQ1*, *PsbQ2*, and *PsbO* genes, which are related to photosynthesis and chloroplast synthesis, incubated *N. benthamiana* with NIR-CDs were increased 48-fold, 32-fold, 148.3%, 246.7%, 90.3%, 98.4%, and 294.4% respectively, as compared to the control treated with equivalent ultrapure water.<sup>103</sup> Li *et al.* synthesized nitrogen and magnesium co-doped carbon dots (Mg, N-CDs) through a one-step hydrothermal method. Exposure of rice seedlings to 300  $\mu$ g per mL Mg, N-CD solution induced significant upregulation of key chlorophyll metabolism genes: Mg-dechelatase subunits (ChlI and ChlD) increased by 93.55% and 15.26%, respectively, while chlorophyll synthase (ChlG) and chlorophyllase-2 demonstrated 115.02% and 29.75% elevation in expression levels. These findings demonstrate that Mg, N-CDs treatment enhances chlorophyll biosynthesis and metabolic activity in rice by modulating the transcriptional regulation of chlorophyll-related enzymes, ultimately leading to improved chlorophyll bioactivity and accumulation.<sup>121</sup> Kou *et al.* demonstrated that tomato seedlings exposed to 0.066 mg per mL CDs exhibited marked upregulation of aquaporin-associated genes in root tissues, with expression levels of *Slaqp2*, *SlPIP2;5*, and *SlTIP2;1* increasing by 3.2-, 2.8-, and 4.1-fold, respectively. This transcriptional activation was correlated with enhanced absorption efficiency of water and essential elements ( $Ca^{2+}$ ,  $Mg^{2+}$ ,  $Mn^{2+}$ ), subsequently leading to a 38.7% elevation in leaf chlorophyll content compared with untreated controls. It is proposed that CD-mediated aquaporin regulation may orchestrate nutrient–water dynamics, thereby optimizing chlorophyll biosynthesis in solanaceous crops.<sup>122</sup>

#### 4.2 Light conversion film and LEDs in controlled-environment agriculture

Vertical farming operates within a controlled environment, enabling year-round food production independent of seasonal or external climatic constraints. This system demonstrates significant potential to sustainably yield high-quality agricultural products by minimizing pesticide and synthetic fertilizer inputs, while concurrently reducing land occupancy and water consumption. Consequently, it emerges as a strategic solution to critical global challenges, including the imbalance between population growth and arable land depletion, as well as food scarcity.<sup>123,124</sup> LEDs are extensively regarded as an alternative to traditional light sources in vertical farming due to the advantage of low energy consumption, high efficiency, narrow spectrum accurately matched with photoreceptors, and protection against pathogen challenge.<sup>125,126</sup> CDs, as a new environment-friendly, cost-effective, and tunable-fluorescence material, are promising alternatives for expensive rare-earth phosphors and toxic metal-based semiconductor quantum dots.<sup>127</sup> Wang *et al.* constructed LEDs by assembling dual-emitting core–shell CDs



(blue-emitting) and a  $\text{CaAlSiN}_3:\text{Eu}^{2+}$  (red-emitting) phosphor into UV-LED chips. When used as an artificial light source for indoor planting, these novel LEDs significantly promoted the growth of lettuce and garland chrysanthemum compared to commercial white LED lamps. This superior performance is attributed to the LED's electroluminescence spectrum, which features two prominent emission bands (470 nm and 612 nm). These bands accurately match the wavelengths most efficiently utilized for photosynthesis, thereby resulting in improved chlorophyll content and enhanced photosynthetic efficiency.<sup>128</sup> Besides, He *et al.* prepared double CD-based fluorescent materials with dual characteristic peaks at 420 nm and 630 nm, accomplished by assembly with blue- and red-emitted CDs into mesoporous alumina and demonstrated that WLEDs fabricated by encapsulation of CD-based fluorescent materials and UV-LED chip were a suitable artificial light source for indoor agriculture.<sup>129</sup>

Beyond the controlled environments of vertical farming, CDs also show great promise in enhancing natural sunlight utilization for protected agriculture in greenhouses. A key technology in this area is the agricultural light conversion film, composed of a light conversion agent and matrix, which is a potential functional material to improve the utilization rate of solar energy and, in turn, increase the yield of crops.<sup>130</sup> The traditional conversion agents, including fluorescent dyes, organic rare-earth complexes, and inorganic rare-earth complexes, are featured by high cost, poor light stability, and low biocompatibility, limiting their practical agricultural application.<sup>131</sup> You *et al.* innovatively synthesized transparent, homogeneous, eco-friendly light conversion film by dispersing CDs into carboxymethyl cellulose aqueous solution, converting UV light to blue light that could be absorbed by photosynthetic pigments.<sup>132</sup> The antioxidative light conversion film prepared by Li *et al.* was fabricated with red emissive carbon dots (RCDs) of high quantum yield (78.3% in *N,N*-dimethylformamide). These RCDs can absorb UV and yellowish green light to emit red light (550–800 nm) and exhibit up-conversion luminescence properties.

Ascorbic acid was added as an antioxidant to inhibit the fluorescence quenching caused by oxidative damage to the RCDs' surface. This technology increased the fresh weight, dry weight, and chlorophyll *a* content of mung bean sprouts by 10.4%, 13.9%, and 7.1%, respectively.<sup>133</sup> Jiang *et al.* developed a novel photoconversion film by assembling down-conversion CDs and up-conversion nanoparticles ( $\text{NaYF}_4:\text{Yb}$ ,  $\text{Tm}@\text{NaYF}_4$ ) to make carboxymethylcellulose (CMC), as shown in Fig. 6. The film has excellent optical transparency in the visible region and strong absorption in the ultraviolet and near-infrared regions. Compared with the control group without the composite membrane, the potential maximum photochemical efficiency of the photosystem II was increased by about 12% compared with that of *Arabidopsis* plants exposed to natural light. This fully demonstrates the effectiveness of CD light-harvesting film in enhancing photosynthesis in agriculture.<sup>134</sup>

#### 4.3 Nanosensors for agriculture

The inherent fluorescence properties, biocompatibility, and easy functionalization of CDs set the tone for the preparation of novel probes or sensors, which can then be used to detect the residues of metals, antibiotics, plant hormones, and other substances in agricultural production.<sup>135–137</sup>

Thakuri *et al.* reported a reaction-driven sensing assembly based on CDs,  $\text{MnO}_2$  nanosheets, and hydroquinone monothiocarbonate (HQTC) for the detection of  $\text{Hg}^{2+}$  ionic contamination. As shown in Fig. 7a, utilizing the lipophilicity of  $\text{Hg}^{2+}$ , the HQTC was induced by mercury ions to be converted to hydroquinone (HQ). HQ, as a reducing agent, reacts with  $\text{MnO}_2$  nanosheets to decompose them, and the originally quenched CDs are re-exposed and release their intrinsic blue fluorescence, thus achieving the purpose of detecting  $\text{Hg}^{2+}$ .<sup>138</sup> Du *et al.* demonstrated the development of CD-based nanosensors synthesized from agricultural crop straw as carbon precursors. The surface-engineered CDs possess abundant carboxyl ( $-\text{COOH}$ ) and amino ( $-\text{NH}_2$ ) functional groups that enable effective coordination with  $\text{Fe}^{3+}$  ions through chelation interactions. This specific coordination induces fluorescence quenching, which exhibits concentration-dependent characteristics proportional to  $\text{Fe}^{3+}$  levels.<sup>139</sup> Gao *et al.* synthesized a novel fluorescent complex (CDs@ZIF-L) as an effective fluorescent probe for the selective detection of  $\text{Fe}^{3+}$  in fruit samples by encapsulating CDs into zeolitic imidazolate frameworks (ZIFs) with a two-dimensional leaf-like structure. Unlike the amorphous CDs reported by Du, the two-dimensional leaf-shaped nanosheet (ZIF-L) not only maintained the structural integrity but also possessed a permeable pore structure, which can enhance the detection sensitivity through the strong adsorption capacity of this metal–organic framework. The fluorescence of CDs@ZIF-L was efficiently quenched in the presence of  $\text{Fe}^{3+}$  at the excitation wavelength of 350 nm, enabling the detection of  $\text{Fe}^{3+}$  in real samples and showing great potential for agricultural pollutant control.<sup>140</sup>

Beyond detecting metals, CD-based nanosensors are equally effective for monitoring a wide range of other agricultural contaminants. Sulfites and bisulfites ( $\text{SO}_3^{2-}$  and  $\text{HSO}_3^-$ ),

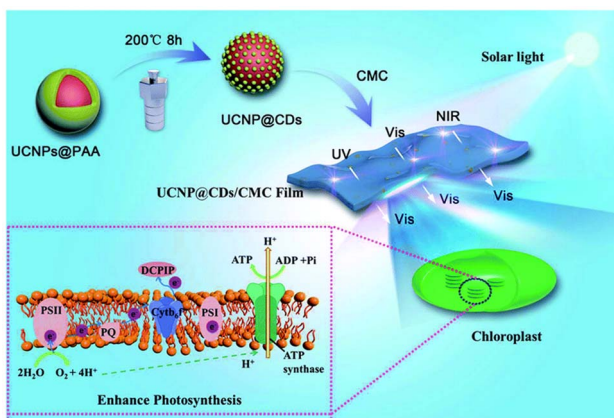


Fig. 6 Illustration of strategy for augmenting natural photosynthesis using light-harvesting films with photo up- and down-conversion properties. Reproduced from ref. 134 with permission from RSC, copyright 2021.



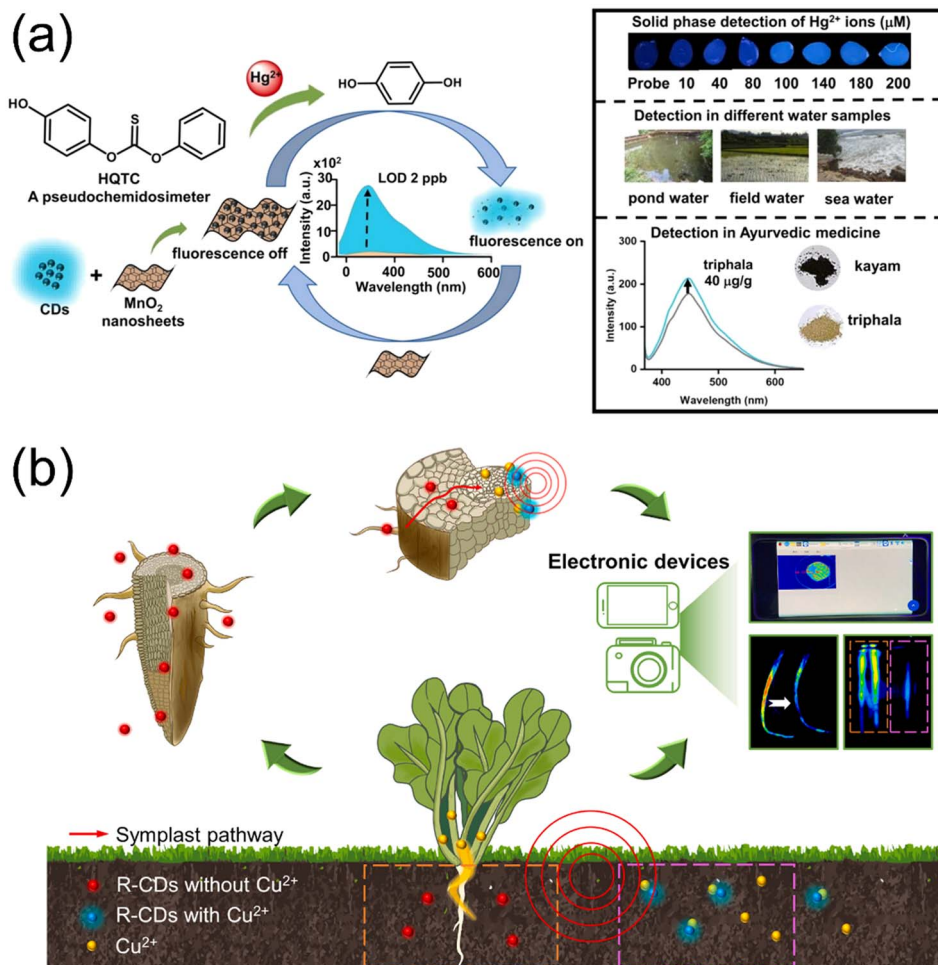


Fig. 7 (a) A reaction-driven sensing assembly based on CDs, MnO<sub>2</sub> nanosheets, and hydroquinone monothiocarbonate (HQTC) for the detection of Hg<sup>2+</sup> ions. Reproduced from ref. 138 with permission from Elsevier, copyright 2024. (b) Schematic diagram of the sensing platform for detecting Cu<sup>2+</sup> within plants and the environment. R-CDs and Cu<sup>2+</sup> can be translocated into the plant systems *via* the symplast pathway, which induces fluorescence quenching of R-CDs upon interaction. The residual Cu<sup>2+</sup> in the environment can also be detected using R-CDs. Reproduced from ref. 147 with permission from Elsevier, copyright 2023.

introduced in food production and storage, are widely used as bleaching agents and preservatives due to their ability to prevent oxidation, inhibit bacterial growth, and suppress enzymatic reactions. However, excessive levels of these compounds can have adverse effects on human health.<sup>141</sup> He *et al.* developed a novel sensitive fluorescent probe (CDs–AgNPs/H<sub>2</sub>O<sub>2</sub>) for SO<sub>3</sub><sup>2-</sup> and HSO<sub>3</sub><sup>-</sup> based on the internal filtration effect (IFE) between silver nanoparticles (AgNPs) and CDs. The fluorescence of CDs is quenched by AgNPs due to the IFE effect, but H<sub>2</sub>O<sub>2</sub> weakens the IFE and restores the fluorescence due to the oxidation of AgNPs by H<sub>2</sub>O<sub>2</sub>. The presence of SO<sub>3</sub><sup>2-</sup>/HSO<sub>3</sub><sup>-</sup> quenches the fluorescence again due to the redox reaction between SO<sub>3</sub><sup>2-</sup>/HSO<sub>3</sub><sup>-</sup> and H<sub>2</sub>O<sub>2</sub>, and the combination of IFE, and the redox reaction can improve the sensitivity and selectivity of the assay.<sup>142</sup> The widespread application of antibiotics across agricultural sectors, including animal husbandry, crop cultivation, and aquaculture, leads to environmental contamination and poses considerable public health risks. Sensitive and timely detection of antibiotics in various agricultural

environments is therefore critically important for mitigating these risks.<sup>143</sup> Wang *et al.* synthesized a new type of nitrogen-doped carbon dots (N-CDs) derived from *Morus alba* by a hydrothermal method. The N-CDs exhibit bright blue fluorescence, a high quantum yield of 60.99%, and excellent photostability, and are used as fluorescent probes for selective detection of tetracyclines (TCs), including oxytetracycline, doxycycline, and minocycline.<sup>144</sup> In addition, Zheng *et al.* successfully prepared biomass-derived CDs by an ionic liquid hydrothermal method using agricultural waste corn cobs as a carbon source and combined them with AgNPs to construct fluorescent probe CDs@IL-AgNPs for direct detection of H<sub>2</sub>O<sub>2</sub> and indirect sensitive detection of melamine, which provides valuable new ideas for the detection of melamine in dairy products and low-carbon and environmentally friendly treatment of agricultural wastes.<sup>145</sup>

Leveraging their biocompatibility, CDs also enable real-time sensing and imaging within living plants. Ghosh *et al.* synthesized CDs by reacting citric acid and ascorbic acid with



ethylenediamine at 140 °C. This single-step, low-temperature synthesis retained their structural and optical properties while minimizing energy consumption, and the successful conduction and fluorescence emission within lettuce plants demonstrated the potential of CDs as a probe for the *in vivo* visualization of plant tissues.<sup>146</sup> On this basis, Lin *et al.* explored the conduction and real-time detection of divalent copper in plants. CDs were used as optical probes to synthesize Cu<sup>2+</sup>-sensitive R-CDs, which were taken up by plants from roots and transported along the plant vasculature system, and the fluorescence bursts were captured by dynamic imaging of electronic devices and processed by built-in algorithmic programs to achieve the real time visualization of the distribution and intensity of Cu<sup>2+</sup> recorded inside the plant (Fig. 7b). With R-CDs exhibiting a detection limit of 0.375 nM for Cu<sup>2+</sup> in water samples, the sensing platform can visually observe and accurately detect 11.7 mg kg<sup>-1</sup> or less of Cu<sup>2+</sup> in plants, and is also suitable for sensing Cu<sup>2+</sup> in the surrounding environment to determine whether heavy metal contamination is present in the vicinity of plants.<sup>147</sup> Beyond these, CD nanosensors can also be used to detect plant hormones. For instance, as one important plant hormone, indole-3-acetic acid (IAA) plays a key role in promoting cell elongation/division and driving overall plant growth and development. Raval *et al.* synthesized green CDs using an extract of the traditional medicinal plant *Plectranthus scutellarioides*. The synthesized PS-CDs exhibited bright green emission at 530 nm (upon 450 nm excitation) with a quantum yield of 21.7% and good stability lasting over 30 days. This stable, highly fluorescent probe was successfully applied for qualitative detection of the plant hormone IAA in real vegetable samples, demonstrating high sensitivity (limit of detection of 0.0421 μM) and producing results that agreed well with high-performance liquid chromatographic analysis.<sup>136</sup>

## 5. The agricultural ecological safety of CDs

Carbon dots, as a new type of agricultural nanomaterial, have drawn much attention for their potential ecological security issues. For sustainable agricultural applications, it is crucial to assess their interactions with crops, soil microorganisms and ecological processes.

The first aspect of agricultural safety involves designing CDs with low toxicity and biodegradable properties. Li *et al.* demonstrated that certain CDs could be internalized and degraded within rice cells, enhancing the plant's stress resistance without accumulating in the environment.<sup>148</sup> On the other hand, using purely green carbon sources such as *Angelica*, licorice, *Forsythia*, *Artemisia argyi*, *Ginkgo*, green tea, henna, rosemary, tea tree, ginger, and turmeric has gained popularity.<sup>149</sup> These plant-derived CDs minimize their adverse impact on the environment. Most importantly, Pan *et al.* elucidated a degradation pathway where CDs were broken down by ·OH radicals into simple compounds, including carboxylic acids, CO<sub>2</sub>, H<sub>2</sub>O, and NH<sub>4</sub><sup>+</sup>. Crucially, these degradation products were not merely safe but were assimilated by lettuce plants,

leading to increased chlorophyll content and enhanced growth.<sup>150</sup> This positions biodegradable CDs within a circular agricultural economy. However, synthesizing nontoxic or fully biodegradable CDs remains challenging due to cost constraints and difficulties in purification.

The second aspect concerns the impact of CDs, which have already been introduced into the environment. Research indicates that CDs can be compatible with key agricultural ecosystems. For instance, Gagana *et al.* achieved 98% removal of dye from wastewater using synthesized CDs@CeO<sub>2</sub>:3Tb<sup>3+</sup> NCs. Water treated with these nanoparticles showed negligible toxicity and even promoted germination in chickpea seeds (*Cicer arietinum*).<sup>151</sup> Similarly, Beker *et al.* used CDs to remediate water contamination, reporting 78–82% degradation of pollutants and a fourfold reduction in toxicity. Unlike other approaches, their study confirmed that CDs used for pollutant degradation did not harm key environmental microorganisms, preserving bacterial communities vital for soil health.<sup>152</sup> Furthermore, Huang *et al.* applied two types of doped CDs to mine soil. Results showed that low concentrations of nitrogen-phosphorus-doped CDs not only exhibited low biotoxicity but also promoted the enrichment of functional microbial communities such as iron-reducing bacteria, thereby enhancing heavy metal immobilization.<sup>153</sup>

Collectively, current data indicate that green-synthesized, low-dose CDs in plants do not disturb soil microbial guilds and can even enhance physiological or remediation traits. Nevertheless, long-term field studies across multiple cropping seasons are still required before large-scale agronomic deployment.

## 6. Summary and outlook

Despite the considerable progress in existing research on CDs, the understanding of the synthesis methods, PL mechanisms, and their applications in agricultural production is still insufficient, and many major issues remain to be resolved. Here, the challenges and future research directions of CDs in agriculture from aspects such as green large-scale synthesis, transport/interaction mechanisms, and long-term safety in agricultural applications are summarized, as shown in Fig. 8.

The controlled large-scale synthesis of CDs from agricultural wastes faces multiple challenges and is difficult to realize. First, the raw materials of agricultural wastes have complex characteristics, diverse compositions, and high impurity content, which increase the difficulty of extracting and purifying CDs. Secondly, the current technology for the synthesis of CDs from agricultural waste is still immature, and there are still problems in the precise control of reaction conditions, synthesis efficiency, and product quality. At the same time, the cost problem should not be ignored, as the process of extracting and purifying CDs from agricultural wastes may consume a lot of energy and materials, which leads to the high cost of the final product. Finally, environmental factors also pose constraints to the large-scale synthesis of CDs from agricultural wastes, and the pollution that may be generated during the treatment and utilization process, as well as the hazardous substances or wastes that may



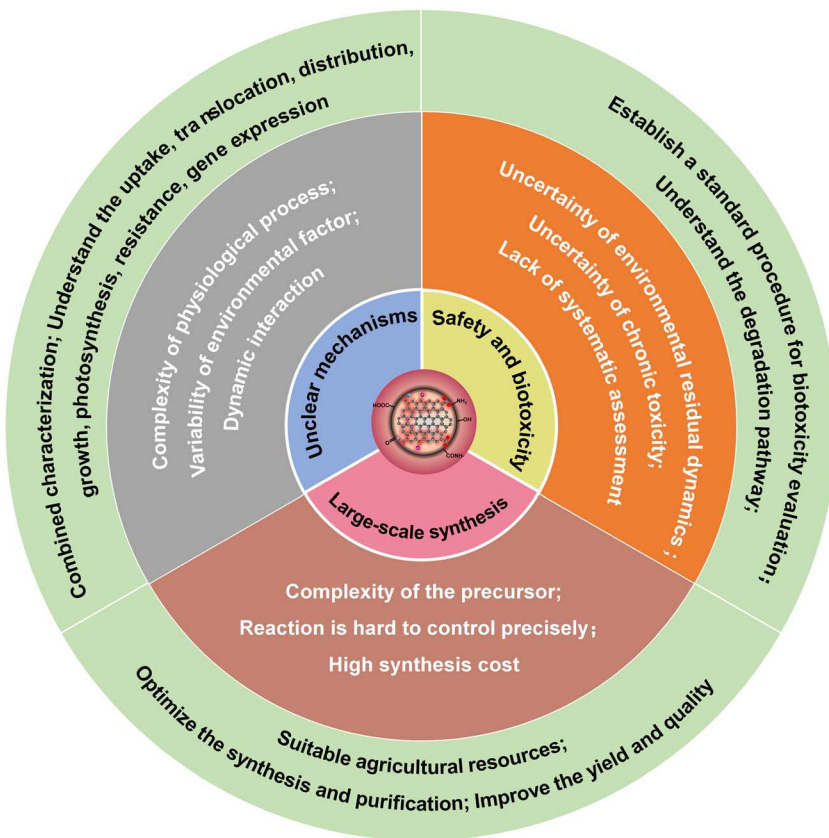


Fig. 8 Challenges and future prospects of CDs in agriculture.

be produced during the synthesis process, needs to be properly dealt with. To realize the controlled large-scale synthesis of CDs from agricultural wastes, researchers should find suitable agricultural resources (raw materials), optimize the synthesis (pyrolysis, hydrothermal/solvothermal, microwave, solid-state carbonization) and purification method/process, reduce the energy consumption, achieve environmentally friendly production, and improve the yield and quality.

Although existing studies have demonstrated that CDs can be transported in the plant body and carry out functions such as sensing,<sup>154–156</sup> drug delivery,<sup>157–159</sup> and promotion of growth and development,<sup>160–162</sup> their transport and mechanism of action in the plant body are unclear, mainly stemming from several challenges. First, the high complexity and diversity of plant physiological processes contribute to the lack of clarity of the transport mechanism of CDs. Secondly, the heterogeneity of CDs in terms of size, morphology, surface charge, and functional groups, induced by divergent synthesis approaches, leads to the poorly understood translocation dynamics in plant systems. Finally, environmental factors such as soil organic matter, mineral elements, pH, as well as light and temperature, may also affect the transport of carbon dots in plants. The complexity and variability of these environmental factors make it difficult to accurately predict and explain the transport process and interaction mechanism. Combined characterization methods such as femtosecond transient absorption, X-ray fluorescence microscopy, steady-state/transient PL

measurements, nondenaturing gel electrophoresis, *in situ* PL, etc., should be utilized to elucidate the uptake, translocation, and distribution of CDs across the plants and gain a deeper understanding of their effects on the plant growth, photosynthesis efficiency, nutritional quality, resistance against environmental stresses, gene expression and so on.

Currently, significant challenges persist in ensuring the long-term safety and minimizing the biotoxicity of CDs in agricultural applications. Existing studies demonstrate that CDs exhibit significant biphasic concentration dependence – low doses promote crop growth while high concentrations inhibit development – with toxicity thresholds modulated by complex interactions between surface chemistry and plant species specificity.<sup>163,164</sup> Simultaneously, CDs can enter the food chain *via* plant uptake, accumulating in organisms and posing risks of potential organ damage, yet systematic assessment of human health impacts under chronic exposure remains lacking. Crucially, knowledge gaps persist regarding CDs' environmental residual dynamics, chronic toxicity of degradation products, and long-term interference with soil microbial community structure and function under continuous application.<sup>165–167</sup> These challenges imperatively require establishing a cross-scale standard procedure for the biotoxicity evaluation of CDs to investigate the degradation pathways, quantify environmental fate, metabolic pathways, and ecological effects, thereby developing a risk management system that balances agricultural efficiency with ecological sustainability



and utilizes the CDs safely in agriculture for the long term. In light of this, the European Union has explicitly mandated under its Plant Protection Products Regulation (EC) No 1107/2009 and Fertilizing Products Regulation (EU) 2019/1009 that pesticides and fertilizers containing nanomaterials must undergo separate risk assessments. Carbon Removal Certification Framework (CRCF) focuses on carbon storage, and its certification concepts and standards offer valuable references for future quantitative assessments of the environmental benefits of nanomaterial applications in agriculture. China is also actively building foundational evaluation mechanisms, such as developing a benchmark database for agricultural product carbon footprint factors. This initiative aims to accurately quantify carbon emissions at each stage of agricultural production, thereby providing essential data support for assessing the emission reduction benefits of nanomaterial applications. The use of CDs in agriculture remains at an early research stage and has not yet entered large-scale commercialization. As a result, it has not triggered mandatory regulatory approval processes. In the future, safety evaluations should advance in parallel with regulatory development to ensure the compliance and sustainable deployment of CDs.

Although CDs are far from being fully utilized and still present the above challenges, they have made considerable progress after over a decade of development. Compared with other carbon nanomaterials, CDs have a wide range of unique advantages, such as excellent fluorescence properties, good biocompatibility, easy functionalization, and simple preparation, making them a significant potential for agricultural production applications. It can be foreseen that the controlled large-scale synthesis of agricultural waste, in-depth research on its transport mechanism, and further studies on its long-term safety and minimization of biological toxicity will greatly promote the wider application of CDs. Looking forward, translating CDs from promising nanomaterials into effective agricultural tools will require interdisciplinary collaboration. Through the synergistic approach – iteratively refining materials based on efficiency and environmental compatibility within sound policies – the potential of CDs for sustainable agriculture can be fully and responsibly realized.

## Conflicts of interest

There are no conflicts to declare.

## Data availability

The data discussed herein can be found in the referenced articles.

## Acknowledgements

This work was financially supported by the Natural Science Foundation of Wuhan (Grant No. 2024040801020301), the Hubei Provincial Natural Science Foundation of China (Grant No. 2024AFB718), and the Fundamental Research Funds for the

Central Universities (Grant No. 2662025GXPY001, 2662024JC004, 2662024GXQD001, and 2662023LXPY006).

## References

- 1 X. Xu, R. Ray, Y. Gu, H. J. Ploehn, L. Gearheart, K. Raker and W. A. Scrivens, Electrophoretic Analysis and Purification of Fluorescent Single-Walled Carbon Nanotube Fragments, *J. Am. Chem. Soc.*, 2004, **126**, 12736–12737.
- 2 S. Zhu, Y. Song, X. Zhao, J. Shao, J. Zhang and B. Yang, The photoluminescence mechanism in carbon dots (graphene quantum dots, carbon nanodots, and polymer dots): current state and future perspective, *Nano Res.*, 2015, **8**, 355–381.
- 3 S. Li, L. Li, H. Tu, H. Zhang, D. S. Silvester, C. E. Banks, G. Zou, H. Hou and X. Ji, The development of carbon dots: from the perspective of materials chemistry, *Mater. Today*, 2021, **51**, 188–207.
- 4 L. Ai, R. Shi, J. Yang, K. Zhang, T. Zhang and S. Lu, Efficient Combination of G-C3N4 and CDs for Enhanced Photocatalytic Performance: A Review of Synthesis, Strategies, and Applications, *Small*, 2021, **17**, 2007523.
- 5 C. Xia, S. Zhu, T. Feng, M. Yang and B. Yang, Evolution and Synthesis of Carbon Dots: From Carbon Dots to Carbonized Polymer Dots, *Adv. Sci.*, 2019, **6**, 1901316.
- 6 T. Bhoyar, N. Saraswat, M. V. Jyothirmai, A. Gupta, S. K. Malla, J. Park, D. Vidyasagar and S. S. Umare, Nitrogen-Doped Graphitic Carbon Dots Embedded in Carbon Nitride Scaffolds for Water Decontamination, *ACS Appl. Nano Mater.*, 2023, **6**, 3484–3496.
- 7 X. Zhang, Y. Liu, C.-H. Kuan, L. Tang, T. D. Krueger, S. Yeasmin, A. Ullah, C. Fang and L.-J. Cheng, Highly fluorescent nitrogen-doped carbon dots with large Stokes shifts, *J. Mater. Chem. C*, 2023, **11**, 11476–11485.
- 8 Z. Ren, J. Wang, C. Xue, M. Deng, H. Yu, T. Lin, J. Zheng, R. He, X. Wang and J. Li, Ultrahighly Sensitive and Selective Glutathione Sensor Based on Carbon Dot-Functionalized Solution-Gate Graphene Transistor, *Anal. Chem.*, 2023, **95**, 17750–17758.
- 9 M. Du, C. Wang, X. Liu, X. Ding and C. Xiang, Morphological insights into uncompetitive fluorescence of coal-based carbon dots and strategies for improvement, *Carbon*, 2024, **228**, 119396.
- 10 S. Khodabakhshi, P. F. Fulvio, K. S. Walton, S. Kiani, Y. Niu, R. E. Palmer, A. R. Barron and E. Andreoli, High surface area microporous carbon nanocubes from controlled processing of graphene oxide nanoribbons, *Carbon*, 2024, **221**, 118940.
- 11 G.-D. Yang, Z. Wang, S.-M. Zhou, T. Wang, J. Yang and H.-Z. Sun, Regulation of fiber surface nucleation kinetics via ordered nitrogen-rich carbon dots, *Chem. Eng. J.*, 2024, **492**, 152087.
- 12 H. Wang, X. Xie, D. Lin, J. Zhou, L. Zhang, Z. Xing, Q. Zhang and L. Xia, Stimuli-responsive carbon nanotubes based on the interlinkage of carbon dots, *Chem. Eng. J.*, 2024, **500**, 156854.



13 M. Shahab, I. Ahmad, N. Nazeef, F. Raziq, S. Ali, B. Khan, M. Khan, A. U. Rahman, K. Zaman, M. Ibrahim, I. Muhammad, I. Ullah, M. Ikram and A. Ali, Casein carbon dots decorated multi-walled carbon nanotubes double matrix supported potassium intercalated manganese oxide for high performance aqueous asymmetric pseudo-super capacitor, *J. Energy Storage*, 2024, **97**, 112879.

14 H. Guo, X. Qu, B. Xing, H. Zeng, W. Kang, S. Cheng, Y. Xing, J. He and C. Zhang, A surface-induced assembly strategy to fabricate flexible carbon nanofiber/coal-based carbon dots films as free-standing anodes for high-performance sodium-ion batteries, *Appl. Surf. Sci.*, 2024, **660**, 159999.

15 Y. Huang, X. Hu, Y. Li, X. Zhong, Z. He, Z. Geng, S. Gan, W. Deng, G. Zou, H. Hou and X. Ji, Demystifying the Influence of Precursor Structure on S-Doped Hard Carbon Anode: Taking Glucose, Carbon Dots, and Carbon Fibers as Examples, *Adv. Funct. Mater.*, 2024, **34**, 2403648.

16 S. Treepet, T. Duangmanee, C. Chokradjaroen, K. Kim, N. Saito and A. Watthanaphanit, Solution plasma synthesis of nitrogen-doped carbon dots from glucosamines: comparative fluorescence modulation for dopamine detection, *Carbon*, 2025, **231**, 119705.

17 P. Zhang, Y. Zheng, L. Ren, S. Li, M. Feng, Q. Zhang, R. Qi, Z. Qin, J. Zhang and L. Jiang, The Enhanced Photoluminescence Properties of Carbon Dots Derived from Glucose: The Effect of Natural Oxidation, *Nanomaterials*, 2024, **14**, 970.

18 Y. Liu, C. Huang, W. Yue, X. Wang, Y. Sun, W. Bi, L. Wang and Y. Xu, Sugar-coated cannonballs for effective antibacterial treatments but with negligible cytotoxicity based on silver (copper) -containing carbon dots and their mechanism analysis, *Carbon*, 2024, **224**, 119085.

19 M. J. Khan, S. Sawatdee, M. Suksaard, Y. Nantarattikul, A. Botalo, N. Juntree, P. Pongchaikul, P. Arjfuk, P. Khemthong, W. Wanmolee, N. Chanlek, N. Laosiripojana, K. C. W. Wu and C. Sakdaronnarong, Ultrafast magneto-inductive synthesis of carbon dots from plant-based precursors using deep eutectic solvents: a comparative study with traditional hydrothermal methods, *Process Saf. Environ. Prot.*, 2025, **195**, 106752.

20 Q. Yuan, M. Fan, Y. Zhao, J. Wu, J. Raj, Z. Wang, A. Wang, H. Sun, X. Xu, Y. Wu, K. Sun and J. Jiang, Facile fabrication of carbon dots containing abundant h-BN/graphite heterostructures as efficient electrocatalyst for hydrogen peroxide synthesis, *Appl. Catal., B*, 2023, **324**, 122195.

21 Y. Hu, O. Seivert, Y. Tang, H. E. Karahan and A. Bianco, Carbon Dot Synthesis and Purification: Trends, Challenges and Recommendations, *Angew. Chem., Int. Ed.*, 2024, **63**, e202412341.

22 N. Tarannum, K. Pooja, M. Singh and A. Panwar, A study on the development of C-dots via green chemistry: a state-of-the-art review, *Carbon Lett.*, 2024, **34**, 1537–1568.

23 J. De Gregori da Rocha, M. B. S. Junior, D. L. P. Macuvele, H. G. Riella, J. L. Ienczak, N. Padoin and C. Soares, Uncovering engineering and mechanistic insights in green synthesis of carbon dots from rice husks, *Chem. Eng. J.*, 2025, **505**, 159364.

24 H. Liu, X. Zhong, Q. Pan, Y. Zhang, W. Deng, G. Zou, H. Hou and X. Ji, A review of carbon dots in synthesis strategy, *Coord. Chem. Rev.*, 2024, **498**, 215468.

25 K.-F. Xu, Z. Wang, M. Cui, Y. Jiang, C. Li, Z.-X. Wang, L.-Y. Li, C. Jia, L. Zhang and F.-G. Wu, Turning Waste into Treasure: Functionalized Biomass-Derived Carbon Dots for Superselective Visualization and Eradication of Gram-Positive Bacteria, *Adv. Sci.*, 2025, **12**, 2411084.

26 Y. Shi, Y. Xia, M. Zhou, Y. Wang, J. Bao, Y. Zhang and J. Cheng, Facile synthesis of Gd/Ru-doped fluorescent carbon dots for fluorescent/MR bimodal imaging and tumor therapy, *J. Nanobiotechnol.*, 2024, **22**, 88.

27 J. Li, X. Zhao and X. Gong, The Emerging Star of Carbon Luminescent Materials: Exploring the Mysteries of the Nanolight of Carbon Dots for Optoelectronic Applications, *Small*, 2024, **20**, 2400107.

28 N. Jayaprakash, K. Elumalai, S. Manickam, G. Bakthavatchalam and P. Tamilselvan, Carbon nanomaterials: revolutionizing biomedical applications with promising potential, *Nano Mater. Sci.*, 2024, **11**, 004.

29 N. Sharma, A. Sharma and H.-J. Lee, The antioxidant properties of green carbon dots: a review, *Environ. Chem. Lett.*, 2025, **23**, 1061–1109.

30 W. Shi, Q. Han, J. Wu, C. Ji, Y. Zhou, S. Li, L. Gao, R. M. Leblanc and Z. Peng, Synthesis Mechanisms, Structural Models, and Photothermal Therapy Applications of Top-Down Carbon Dots from Carbon Powder, Graphite, Graphene, and Carbon Nanotubes, *Int. J. Mol. Sci.*, 2022, **23**, 1456.

31 W. Chen, G. Lv, W. Hu, D. Li, S. Chen and Z. Dai, Synthesis and applications of graphene quantum dots: a review, *Nanotechnol. Rev.*, 2018, **7**, 157–185.

32 H. Li, J. Huang, Y. Liu, F. Lu, J. Zhong, Y. Wang, S. Li, Y. Lifshitz, S.-T. Lee and Z. Kang, Enhanced RuBisCO activity and promoted dicotyledons growth with degradable carbon dots, *Nano Res.*, 2019, **12**, 1585–1593.

33 J. A. Ferreira, L. L. Name, L. C. Lieb, D. Y. Tiba, M. M. da Silva, A. C. Oliveira and T. C. Canevari, Carbon Dots Hybrid Nanostructure-based Electrochemical Sensors: Applications in Determining Different Species in a Real Sample, *Curr. Nanosci.*, 2024, **20**, 31–46.

34 B. A. R. Suganthi, J. T. Anandhi, M. A. Francis, G. Sudha, U. R. Josephine UR and K. Hema, Green Synthesis of Carbon Dots: Advancements, Characterization, and Emerging Biological Applications, *J. Fluoresc.*, 2025, **2**, DOI: [10.1007/s10895-025-04428-2](https://doi.org/10.1007/s10895-025-04428-2).

35 T. N. Anh, N. T. Hien, H.-L. T. Dang, N. T. B. Ngoc, P. T. Dien, N. M. Hoang, N. T. Hanh, N. T. Ha, N. M. Khai, T. D. Pham and V.-D. Dao, Green chemistry for synthesizing carbon dots and their application in pollutant treatment and environmental protection, *Desalination*, 2025, **615**, 119214.

36 Z. Bian, E. Gomez, M. Gruebele, B. G. Levine, S. Link, A. Mehmood and S. Nie, Bottom-up carbon dots:



purification, single-particle dynamics, and electronic structure, *Chem. Sci.*, 2025, **16**, 4195–4212.

37 H. Pei, Z. Zhang, M. Ouyang, H. Liang, J. Liu, S. Li, H. Zhang, Y. Qi, L. Wei, C. Liu, L. Shi, R. Guo, N. Liu and Z. Mo, Chiral carbonized polymer dots: a comprehensive review, *Sustainable Mater. Technol.*, 2025, **43**, e01271.

38 H. Liu, T. Ye and C. Mao, Fluorescent carbon nanoparticles derived from candle soot, *Angew. Chem.*, 2007, **119**, 6593–6595.

39 X. Zhou, Y. Zhang, C. Wang, X. Wu, Y. Yang, B. Zheng, H. Wu, S. Guo and J. Zhang, Photo-Fenton Reaction of Graphene Oxide: A New Strategy to Prepare Graphene Quantum Dots for DNA Cleavage, *ACS Nano*, 2012, **6**, 6592–6599.

40 J. Zhou, C. Booker, R. Li, X. Zhou, T.-K. Sham, X. Sun and Z. Ding, An Electrochemical Avenue to Blue Luminescent Nanocrystals from Multiwalled Carbon Nanotubes (MWCNTs), *J. Am. Chem. Soc.*, 2007, **129**, 744–745.

41 M. He, X. Guo, J. Huang, H. Shen, Q. Zeng and L. Wang, Mass production of tunable multicolor graphene quantum dots from an energy resource of coke by a one-step electrochemical exfoliation, *Carbon*, 2018, **140**, 508–520.

42 T. Zhang, H. Zhao, G. Fan, Y. Li, L. Li and X. Quan, Electrolytic exfoliation synthesis of boron doped graphene quantum dots: a new luminescent material for electrochemiluminescence detection of oncogene microRNA-20a, *Electrochim. Acta*, 2016, **190**, 1150–1158.

43 J. Deng, Q. Lu, N. Mi, H. Li, M. Liu, M. Xu, L. Tan, Q. Xie, Y. Zhang and S. Yao, Electrochemical Synthesis of Carbon Nanodots Directly from Alcohols, *Chem.-Eur. J.*, 2014, **20**, 4993–4999.

44 Y.-P. Sun, B. Zhou, Y. Lin, W. Wang, K. A. S. Fernando, P. Pathak, M. J. Meziani, B. A. Harruff, X. Wang, H. Wang, P. G. Luo, H. Yang, M. E. Kose, B. Chen, L. M. Veca and S.-Y. Xie, Quantum-Sized Carbon Dots for Bright and Colorful Photoluminescence, *J. Am. Chem. Soc.*, 2006, **128**, 7756–7757.

45 S. H. Kang, S. Mhin, H. Han, K. M. Kim, J. L. Jones, J. H. Ryu, J. S. Kang, S. H. Kim and K. B. Shim, Ultrafast Method for Selective Design of Graphene Quantum Dots with Highly Efficient Blue Emission, *Sci. Rep.*, 2016, **6**, 38423.

46 Z. Hallaji, Z. Bagheri, Z. Tavassoli and B. Ranjbar, Fluorescent carbon dot as an optical amplifier in modern agriculture, *Sustainable Mater. Technol.*, 2022, **34**, e00493.

47 B. Zhang, C.-y. Liu and Y. Liu, A Novel One-Step Approach to Synthesize Fluorescent Carbon Nanoparticles, *Eur. J. Inorg. Chem.*, 2010, **2010**, 4411–4414.

48 L. Lu, Y. Zhu, C. Shi and Y. T. Pei, Large-scale synthesis of defect-selective graphene quantum dots by ultrasonic-assisted liquid-phase exfoliation, *Carbon*, 2016, **109**, 373–383.

49 X. Miao, D. Qu, D. Yang, B. Nie, Y. Zhao, H. Fan and Z. Sun, Synthesis of Carbon Dots with Multiple Color Emission by Controlled Graphitization and Surface Functionalization, *Adv. Mater.*, 2018, **30**, 1704740.

50 P. Zhu, J. Li, L. Gao, J. Xiong and K. Tan, Strategy to Synthesize Tunable Multiemission Carbon Dots and Their Multicolor Visualization Application, *ACS Appl. Mater. Interfaces*, 2021, **13**, 33354–33362.

51 A. Tan, G. Yang and X. Wan, Ultra-high quantum yield nitrogen-doped carbon quantum dots and their versatile application in fluorescence sensing, bioimaging and anti-counterfeiting, *Spectrochim. Acta, Part A*, 2021, **253**, 119583.

52 C. Ji, Q. Han, Y. Zhou, J. Wu, W. Shi, L. Gao, R. M. Leblanc and Z. Peng, Phenylenediamine-derived near infrared carbon dots: the kilogram-scale preparation, formation process, photoluminescence tuning mechanism and application as red phosphors, *Carbon*, 2022, **192**, 198–208.

53 D. Sun, T. Liu, C. Wang, L. Yang, S. Yang and K. Zhuo, Hydrothermal synthesis of fluorescent carbon dots from gardenia fruit for sensitive on-off-on detection of  $Hg^{2+}$  and cysteine, *Spectrochim. Acta, Part A*, 2020, **240**, 118598.

54 S. A. A. Vandarkuzhali, V. Jeyalakshmi, G. Sivaraman, S. Singaravelivel, K. R. Krishnamurthy and B. Viswanathan, Highly fluorescent carbon dots from Pseudo-stem of banana plant: applications as nanosensor and bio-imaging agents, *Sens. Actuators, B*, 2017, **252**, 894–900.

55 Z. Li, Q. Wang, Z. Zhou, S. Zhao, S. Zhong, L. Xu, Y. Gao and X. Cui, Green synthesis of carbon quantum dots from corn stalk shell by hydrothermal approach in near-critical water and applications in detecting and bioimaging, *Microchem. J.*, 2021, **166**, 106250.

56 M. Rong, Y. Feng, Y. Wang and X. Chen, One-pot solid phase pyrolysis synthesis of nitrogen-doped carbon dots for  $Fe^{3+}$  sensing and bioimaging, *Sens. Actuators, B*, 2017, **245**, 868–874.

57 S. F. El-Malla, E. A. Elshenawy, S. F. Hammad and F. R. Mansour, Rapid microwave synthesis of N,S-doped carbon quantum dots as a novel turn off-on sensor for label-free determination of copper and etidronate disodium, *Anal. Chim. Acta*, 2022, **1197**, 339491.

58 P. Yang, Z. Zhu, X. Li, T. Zhang, W. Zhang, M. Chen and X. Zhou, Facile synthesis of yellow emissive carbon dots with high quantum yield and their application in construction of fluorescence-labeled shape memory nanocomposite, *J. Alloys Compd.*, 2020, **834**, 154399.

59 N. K. Sahoo, G. C. Jana, M. N. Aktara, S. Das, S. Nayim, A. Patra, P. Bhattacharjee, K. Bhadra and M. Hossain, Carbon dots derived from lychee waste: application for  $Fe^{3+}$  ions sensing in real water and multicolor cell imaging of skin melanoma cells, *Mater. Sci. Eng. C*, 2020, **108**, 110429.

60 F. Wang, S. Pang, L. Wang, Q. Li, M. Kreiter and C.-y. Liu, One-Step Synthesis of Highly Luminescent Carbon Dots in Noncoordinating Solvents, *Chem. Mater.*, 2010, **22**, 4528–4530.

61 M. J. Krysman, A. Kelarakis, P. Dallas and E. P. Giannelis, Formation Mechanism of Carbogenic Nanoparticles with Dual Photoluminescence Emission, *J. Am. Chem. Soc.*, 2012, **134**, 747–750.



62 H. Zhang, B. Wang, X. Yu, J. Li, J. Shang and J. Yu, Carbon dots in porous materials: host–guest synergy for enhanced performance, *Angew. Chem.*, 2020, **132**, 19558–19570.

63 Z. G. Gu, D. J. Li, C. Zheng, Y. Kang, C. Wöll and J. Zhang, MOF-templated synthesis of ultrasmall photoluminescent carbon-nanodot arrays for optical applications, *Angew. Chem.*, 2017, **129**, 6957–6962.

64 R. K. Singh, R. Kumar, D. P. Singh, R. Savu and S. A. Moshkalev, Progress in microwave-assisted synthesis of quantum dots (graphene/carbon/semiconducting) for bioapplications: a review, *Mater. Today Chem.*, 2019, **12**, 282–314.

65 H.-J. Wang, W.-Y. Hou, J. Kang, X.-Y. Zhai, H.-L. Chen, Y.-W. Hao and G.-Y. Wan, The facile preparation of solid-state fluorescent carbon dots with a high fluorescence quantum yield and their application in rapid latent fingerprint detection, *Dalton Trans.*, 2021, **50**, 12188–12196.

66 A. Kanwal, N. Bibi, S. Hyder, A. Muhammad, H. Ren, J. Liu and Z. Lei, Recent advances in green carbon dots (2015–2022): synthesis, metal ion sensing, and biological applications, *Beilstein J. Nanotechnol.*, 2022, **13**, 1068–1107.

67 S. Xiang and M. Tan, Carbon dots derived from natural sources and their biological and environmental impacts, *Environ. Sci.: Nano*, 2022, **9**, 3206–3225.

68 F. Yuan, T. Yuan, L. Sui, Z. Wang, Z. Xi, Y. Li, X. Li, L. Fan, Z. a. Tan, A. Chen, M. Jin and S. Yang, Engineering triangular carbon quantum dots with unprecedented narrow bandwidth emission for multicolored LEDs, *Nat. Commun.*, 2018, **9**, 2249.

69 H. Ding, S.-B. Yu, J.-S. Wei and H.-M. Xiong, Full-Color Light-Emitting Carbon Dots with a Surface-State-Controlled Luminescence Mechanism, *ACS Nano*, 2016, **10**, 484–491.

70 M. Wang, R. Sun, Q. Wang, L. Chen, L. Hou, Y. Chi, C. H. Lu, F. Fu and Y. Dong, Effects of C-Related Dangling Bonds and Functional Groups on the Fluorescent and Electrochemiluminescent Properties of Carbon-Based Dots, *Chem.-Eur. J.*, 2018, **24**, 4250–4254.

71 Q. Fang, Y. Dong, Y. Chen, C.-H. Lu, Y. Chi, H.-H. Yang and T. Yu, Luminescence origin of carbon based dots obtained from citric acid and amino group-containing molecules, *Carbon*, 2017, **118**, 319–326.

72 Y. Ding, J. Zheng, J. Wang, Y. Yang and X. Liu, Direct blending of multicolor carbon quantum dots into fluorescent films for white light emitting diodes with an adjustable correlated color temperature, *J. Mater. Chem. C*, 2019, **7**, 1502–1509.

73 Y. Song, S. Zhu, S. Zhang, Y. Fu, L. Wang, X. Zhao and B. Yang, Investigation from chemical structure to photoluminescent mechanism: a type of carbon dots from the pyrolysis of citric acid and an amine, *J. Mater. Chem. C*, 2015, **3**, 5976–5984.

74 L. Ai, Y. Yang, B. Wang, J. Chang, Z. Tang, B. Yang and S. Lu, Insights into photoluminescence mechanisms of carbon dots: advances and perspectives, *Sci. Bull.*, 2021, **66**, 839–856.

75 H. Li, X. He, Z. Kang, H. Huang, Y. Liu, J. Liu, S. Lian, C. H. Tsang, X. Yang and S. T. Lee, Water-soluble fluorescent carbon quantum dots and photocatalyst design, *Angew. Chem. Int. Ed. Engl.*, 2010, **49**, 4430–4434.

76 M. A. Sk, A. Ananthanarayanan, L. Huang, K. H. Lim and P. Chen, Revealing the tunable photoluminescence properties of graphene quantum dots, *J. Mater. Chem. C*, 2014, **2**, 6954–6960.

77 T.-F. Yeh, W.-L. Huang, C.-J. Chung, I. T. Chiang, L.-C. Chen, H.-Y. Chang, W.-C. Su, C. Cheng, S.-J. Chen and H. Teng, Elucidating Quantum Confinement in Graphene Oxide Dots Based On Excitation-Wavelength-Independent Photoluminescence, *J. Phys. Chem. Lett.*, 2016, **7**, 2087–2092.

78 B. Wang, J. Yu, L. Sui, S. Zhu, Z. Tang, B. Yang and S. Lu, Rational Design of Multi-Color-Emissive Carbon Dots in a Single Reaction System by Hydrothermal, *Adv. Sci.*, 2021, **8**, 2001453.

79 H. Ding, S. B. Yu, J. S. Wei and H. M. Xiong, Full-Color Light-Emitting Carbon Dots with a Surface-State-Controlled Luminescence Mechanism, *ACS Nano*, 2016, **10**, 484–491.

80 H. Guo, X. Zhang, Z. Chen, L. Zhang, L. Wang, J. Xu and M. Wu, High-energy short-wave blue light conversion films via carbon quantum dots for preventing retinal photochemical damage, *Carbon*, 2022, **199**, 431–438.

81 A. Vibhute, T. Patil, R. Gambhir and A. P. Tiwari, Fluorescent carbon quantum dots: synthesis methods, functionalization and biomedical applications, *Appl. Surf. Sci. Adv.*, 2022, **11**, 100311.

82 K. Wang, J. Dong, L. Sun, H. Chen, Y. Wang, C. Wang and L. Dong, Effects of elemental doping on the photoluminescence properties of graphene quantum dots, *RSC Adv.*, 2016, **6**, 91225–91232.

83 R. Atchudan, T. N. J. I. Edison, S. Perumal, N. Muthuchamy and Y. R. Lee, Hydrophilic nitrogen-doped carbon dots from biowaste using dwarf banana peel for environmental and biological applications, *Fuel*, 2020, **275**, 117821.

84 F. Ehrat, S. Bhattacharyya, J. Schneider, A. Löf, R. Wyrwich, A. L. Rogach, J. K. Stolarczyk, A. S. Urban and J. Feldmann, Tracking the Source of Carbon Dot Photoluminescence: Aromatic Domains versus Molecular Fluorophores, *Nano Lett.*, 2017, **17**, 7710–7716.

85 S. Karami, M. Shamsipur, A. A. Taherpour, M. Jamshidi and A. Barati, In Situ Chromophore Doping: A New Mechanism for the Long-Wavelength Emission of Carbon Dots, *J. Phys. Chem. C*, 2020, **124**, 10638–10646.

86 W. Kasprzyk, T. Świergosz, S. Bednarz, K. Walas, N. V. Bashmakova and D. Bogdał, Luminescence phenomena of carbon dots derived from citric acid and urea – a molecular insight, *Nanoscale*, 2018, **10**, 13889–13894.

87 Y. Gong and J. Zhao, Small Carbon Quantum Dots, Large Photosynthesis Enhancement, *J. Agric. Food Chem.*, 2018, **66**, 9159–9161.



88 C. Li, X. Du and C. Liu, Enhancing crop yields to ensure food security by optimizing photosynthesis, *J. Genet. Genomics*, 2025, **01**, 002.

89 X.-G. Zhu, S. P. Long and D. R. Ort, What is the maximum efficiency with which photosynthesis can convert solar energy into biomass?, *Curr. Opin. Biotechnol.*, 2008, **19**, 153–159.

90 X. G. Zhu, S. P. Long and D. R. Ort, Improving photosynthetic efficiency for greater yield, *Annu. Rev. Plant Biol.*, 2010, **61**, 235–261.

91 P. F. South, A. P. Cavanagh, H. W. Liu and D. R. Ort, Synthetic glycolate metabolism pathways stimulate crop growth and productivity in the field, *Science*, 2019, **363**, eaat9077.

92 G. Chen, K. Jin, J. Wang, Y. Li, X. Tian, L. Zhang, S. Wu, J. Yang, X. Cui, J. Sun, X. Sun, T. Lu and Z. Zhang, Carbon-positive photorespiratory bypass via the tartronyl-coenzyme A pathway enhances carbon fixation efficiency and yield in rice, *Plant Biotechnol. J.*, 2025, **23**, 4712–4714.

93 M. Ermakova, P. E. Lopez-Calcagno, C. A. Raines, R. T. Furbank and S. von Caemmerer, Overexpression of the Rieske FeS protein of the Cytochrome b(6)f complex increases C(4) photosynthesis in *Setaria viridis*, *Commun. Biol.*, 2019, **2**, 314.

94 D. Patel-Tupper, A. Kelikian, A. Leipertz, N. Maryn, M. Tjahjadi, N. G. Karavolias, M.-J. Cho and K. K. Niyogi, Multiplexed CRISPR-Cas9 mutagenesis of rice *PSBS1* noncoding sequences for transgene-free overexpression, *Sci. Adv.*, 2024, **10**, eadm7452.

95 M. Yang, H. Li, X. Liu, L. Huang, B. Zhang, K. Liu, W. Xie, J. Cui, D. Li, L. Lu, H. Sun and B. Yang, Fe-doped carbon dots: a novel biocompatible nanoplatform for multi-level cancer therapy, *J. Nanobiotechnol.*, 2023, **21**, 431.

96 H. Wang, L. Ai, H. Song, Z. Song, X. Yong, S. Qu and S. Lu, Innovations in the Solid-State Fluorescence of Carbon Dots: Strategies, Optical Manipulations, and Applications, *Adv. Funct. Mater.*, 2023, **33**, 2303756.

97 M. Cacioppo, T. Scharl, L. Đorđević, A. Cadranel, F. Arcudi, D. M. Guldi and M. Prato, Symmetry-Breaking Charge-Transfer Chromophore Interactions Supported by Carbon Nanodots, *Angew. Chem., Int. Ed.*, 2020, **59**, 12779–12784.

98 Z.-P. Ye, Nonlinear optical absorption of photosynthetic pigment molecules in leaves, *Photosynth. Res.*, 2012, **112**, 31–37.

99 B. Guo, G. Liu, H. Wei, J. Qiu, J. Zhuang, X. Zhang, M. Zheng, W. Li, H. Zhang, C. Hu, B. Lei and Y. Liu, The role of fluorescent carbon dots in crops: mechanism and applications, *SmartMat*, 2022, **3**, 208–225.

100 E. Budak, D. Erdoğan and C. Ünlü, Enhanced fluorescence of photosynthetic pigments through conjugation with carbon quantum dots, *Photosynth. Res.*, 2021, **147**, 1–10.

101 L. Sai, S. Liu, X. Qian, Y. Yu and X. Xu, Nontoxic fluorescent carbon nanodot serving as a light conversion material in plant for UV light utilization, *Colloids Surf., B*, 2018, **169**, 422–428.

102 D. Li, W. Li, H. Zhang, X. Zhang, J. Zhuang, Y. Liu, C. Hu and B. Lei, Far-Red Carbon Dots as Efficient Light-Harvesting Agents for Enhanced Photosynthesis, *ACS Appl. Mater. Interfaces*, 2020, **12**, 21009–21019.

103 Y. Wang, Z. Xie, X. Wang, X. Peng and J. Zheng, Fluorescent carbon-dots enhance light harvesting and photosynthesis by overexpressing *PsbP* and *PsiK* genes, *J. Nanobiotechnol.*, 2021, **19**, 260.

104 Y. Zhang, E. Kaiser, Y. Zhang, Q. Yang and T. Li, Red/blue light ratio strongly affects steady-state photosynthesis, but hardly affects photosynthetic induction in tomato (*Solanum lycopersicum*), *Physiol. Plant.*, 2019, **167**, 144–158.

105 G. Trouwborst, S. W. Hogewoning, O. van Kooten, J. Harbinson and W. van Ieperen, Plasticity of photosynthesis after the ‘red light syndrome’ in cucumber, *Environ. Exp. Bot.*, 2016, **121**, 75–82.

106 W. Li, S. Wu, H. Zhang, X. Zhang, J. Zhuang, C. Hu, Y. Liu, B. Lei, L. Ma and X. Wang, Enhanced Biological Photosynthetic Efficiency Using Light-Harvesting Engineering with Dual-Emissive Carbon Dots, *Adv. Funct. Mater.*, 2018, **28**, 1804004.

107 W. Li, Y. Zheng, H. Zhang, Z. Liu, W. Su, S. Chen, Y. Liu, J. Zhuang and B. Lei, Phytotoxicity, Uptake, and Translocation of Fluorescent Carbon Dots in Mung Bean Plants, *ACS Appl. Mater. Interfaces*, 2016, **8**, 19939–19945.

108 D. Xiao, M. Jiang, X. Luo, S. Liu, J. Li, Z. Chen and S. Li, Sustainable Carbon Dot-Based AIEgens: Promising Light-Harvesting Materials for Enhancing Photosynthesis, *ACS Sustain. Chem. Eng.*, 2021, **9**, 4139–4145.

109 S. Viola, J. Sellés, B. Bailleul, P. Joliot and F. A. Wollman, In vivo electron donation from plastocyanin and cytochrome c(6) to PSI in *Synechocystis* sp. PCC6803, *Biochim. Biophys. Acta, Bioenerg.*, 2021, **1862**, 148449.

110 A. J. Simkin, L. McAusland, T. Lawson and C. A. Raines, Overexpression of the RieskeFeS Protein Increases Electron Transport Rates and Biomass Yield, *Plant Physiol.*, 2017, **175**, 134–145.

111 S. Chandra, S. Pradhan, S. Mitra, P. Patra, A. Bhattacharya, P. Pramanik and A. Goswami, High throughput electron transfer from carbon dots to chloroplast: a rationale of enhanced photosynthesis, *Nanoscale*, 2014, **6**, 3647–3655.

112 F. Zhao, V. Hartmann, A. Ruff, M. M. Nowaczyk, M. Rögner, W. Schuhmann and F. Conzuelo, Unravelling electron transfer processes at photosystem 2 embedded in an Os-complex modified redox polymer, *Electrochim. Acta*, 2018, **290**, 451–456.

113 J. R. Shen, The Structure of Photosystem II and the Mechanism of Water Oxidation in Photosynthesis, *Annu. Rev. Plant Biol.*, 2015, **66**, 23–48.

114 C. Wang, H. Yang, F. Chen, L. Yue, Z. Wang and B. Xing, Nitrogen-Doped Carbon Dots Increased Light Conversion and Electron Supply to Improve the Corn Photosystem and Yield, *Environ. Sci. Technol.*, 2021, **55**, 12317–12325.

115 K. Ocakoglu, T. Krupnik, B. van den Bosch, E. Harputlu, M. P. Gullo, J. D. J. Olmos, S. Yildirimcan, R. K. Gupta, F. Yakuphanoglu, A. Barbieri, J. N. H. Reek and J. Kargul, Photosystem I-based Biophotovoltaics on Nanostructured Hematite, *Adv. Funct. Mater.*, 2014, **24**, 7467–7477.



116 H. Wang, M. Zhang, Y. Song, H. Li, H. Huang, M. Shao, Y. Liu and Z. Kang, Carbon dots promote the growth and photosynthesis of mung bean sprouts, *Carbon*, 2018, **136**, 94–102.

117 B. Guo, G. Liu, W. Li, C. Hu, B. Lei, J. Zhuang, M. Zheng and Y. Liu, The role of carbon dots in the life cycle of crops, *Ind. Crops Prod.*, 2022, **187**, 115427.

118 C. A. Raines, Increasing Photosynthetic Carbon Assimilation in C3 Plants to Improve Crop Yield: Current and Future Strategies, *Plant Physiol.*, 2011, **155**, 36–42.

119 M. Betti, H. Bauwe, F. A. Busch, A. R. Fernie, O. Keech, M. Levey, D. R. Ort, M. A. Parry, R. Sage, S. Timm, B. Walker and A. P. Weber, Manipulating photorespiration to increase plant productivity: recent advances and perspectives for crop improvement, *J. Exp. Bot.*, 2016, **67**, 2977–2988.

120 M. Zhang, L. Hu, H. Wang, Y. Song, Y. Liu, H. Li, M. Shao, H. Huang and Z. Kang, One-step hydrothermal synthesis of chiral carbon dots and their effects on mung bean plant growth, *Nanoscale*, 2018, **10**, 12734–12742.

121 Y. Li, X. Xu, B. Lei, J. Zhuang, X. Zhang, C. Hu, J. Cui and Y. Liu, Magnesium-nitrogen co-doped carbon dots enhance plant growth through multifunctional regulation in photosynthesis, *Chem. Eng. J.*, 2021, **422**, 130114.

122 E. Kou, Y. Yao, X. Yang, S. Song, W. Li, Y. Kang, S. Qu, R. Dong, X. Pan, D. Li, H. Zhang and B. Lei, Regulation Mechanisms of Carbon Dots in the Development of Lettuce and Tomato, *ACS Sustain. Chem. Eng.*, 2021, **9**, 944–953.

123 S. H. van Delden, M. S. Kumar, M. Butturini, L. J. A. Graamans, E. Heuvelink, M. Kacira, E. Kaiser, R. S. Klamer, L. Klerkx, G. Kootstra, A. Loeber, R. E. Schouten, C. Stanghellini, W. van Ieperen, J. C. Verdonk, S. Vlaet-Chabrand, E. J. Woltering, R. van de Zedde, Y. Zhang and L. F. M. Marcelis, Current status and future challenges in implementing and upscaling vertical farming systems, *Nat. Food*, 2021, **2**, 944–956.

124 Z. Tian, W. Ma, Q. Yang and F. Duan, Application status and challenges of machine vision in plant factory—a review, *Inf. Process. Agric.*, 2022, **9**, 195–211.

125 Z. Zhou, S. Feng, S. Gai, P. Gao, C. Xu, M. Xia, W. Tang and X. Lu, Affordable phosphor-converted LEDs with specific light quality facilitate the tobacco seedling growth with low energy consumption in Industrial Seedling Raising, *J. Photochem. Photobiol., B*, 2022, **235**, 112564.

126 G. Lauria, E. Lo Piccolo, C. Ceccanti, L. Guidi, R. Bernardi, F. Araniti, L. Cotrozzi, E. Pellegrini, M. Moriconi, T. Giordani, C. Pugliesi, C. Nali, L. Sanità di Toppi, L. Paoli, F. Malorgio, P. Vernieri, R. Massai, D. Remorini and M. Landi, Supplemental red LED light promotes plant productivity, “photomodulates” fruit quality and increases *Botrytis cinerea* tolerance in strawberry, *Postharvest Biol. Technol.*, 2023, **198**, 112253.

127 B. Wang and S. Lu, The light of carbon dots: from mechanism to applications, *Matter*, 2022, **5**, 110–149.

128 L. Wang, H. Zhang, X. Zhou, Y. Liu and B. Lei, A dual-emitting core-shell carbon dot–silica–phosphor composite for LED plant grow light, *RSC Adv.*, 2017, **7**, 16662–16667.

129 Y. He, J. He, Z. Yu, H. Zhang, Y. Liu, G. Hu, M. Zheng, H. Dong, J. Zhuang and B. Lei, Double carbon dot assembled mesoporous aluminas: solid-state dual-emission photoluminescence and multifunctional applications, *J. Mater. Chem. C*, 2018, **6**, 2495–2501.

130 Y. Yang, Y. Zhao, Y. Hu, X. Peng and L. Zhong, Xylan-Derived Light Conversion Nanocomposite Film, *Polymers*, 2020, **12**, 1779.

131 Y. Liu, Z. Gui and J. Liu, Research Progress of Light Wavelength Conversion Materials and Their Applications in Functional Agricultural Films, *Polymers*, 2022, **14**, 851.

132 Y. You, H. Zhang, Y. Liu and B. Lei, Transparent sunlight conversion film based on carboxymethyl cellulose and carbon dots, *Carbohydr. Polym.*, 2016, **151**, 245–250.

133 D. Li, E. Kou, W. Li, H. Zhang, X. Zhang, J. Zhuang, Y. Liu, C. Hu, Y. Zheng, Q. Yang and B. Lei, Oxidation-induced quenching mechanism of ultrabright red carbon dots and application in antioxidant RCDs/PVA film, *Chem. Eng. J.*, 2021, **425**, 131653.

134 M. Jiang, Y. Yuan, Y. Fang, S. Liu, J. Li, Z. Chen, Q. Pang and S. Li, Integrating photon up- and down-conversion to produce efficient light-harvesting materials for enhancing natural photosynthesis, *J. Mater. Chem. A*, 2021, **9**, 24308–24314.

135 M. Kuligowska and S. Neffe, Carbon dots as sensors and sorbents in environmental monitoring protection and chemical analysis, *TrAC, Trends Anal. Chem.*, 2024, **176**, 117767.

136 J. B. Raval, V. N. Mehta, S. Jha, T. J. Park and S. K. Kailasa, Synthesis of green emissive *Plectranthus scutellarioides* carbon dots for sustainable and label-free detection of phytohormone indole-3-acetic acid, *Inorg. Chem. Commun.*, 2025, **171**, 113660.

137 M. Jiang, Y. Sun, M. Chen, H. Ji, Y. Liu, R. Qin, X. Li, H. Gao, R. Zhang and L. Zhang, Multicolor luminescence of carbon dots: from mechanisms to applications, *Chem. Eng. J.*, 2024, **496**, 153761.

138 A. Thakuri, A. A. Bhosle, S. D. Hiremath, M. Banerjee and A. Chatterjee, A carbon dots-MnO<sub>2</sub> nanosheet-based turn-on pseudochemodosimeter as low-cost probe for selective detection of hazardous mercury ion contaminations in water, *J. Hazard. Mater.*, 2024, **469**, 133998.

139 Y. Du, Y. Li, Y. Liu, N. Liu, Y. Cheng, Q. Shi, X. Liu, Z. Tao, Y. Guo, J. Zhang, N. Askaria and H. Li, Stalk-derived carbon dots as nanosensors for Fe<sup>3+</sup> ions detection and biological cell imaging, *Front. Bioeng. Biotechnol.*, 2023, **11**, 2023.

140 M. Gao, G. Liu, Q. Tan, C. Zhao, G. Chen, R. Zhai, Y. Hua, X. Huang, J. Wang and D. Xu, A novel fluorescent probe for Fe<sup>3+</sup> detection based on two-dimensional leaf-like structure CDs@ZIF-L, *Microchem. J.*, 2022, **182**, 107868.

141 S. Assoi, A. M. Niamké, N. G. Y. Konan, M. Cissé and B. S. B. Bamba, Effects of two different pretreatment methods on the nutritional composition, antioxidant capacity, and functional properties of mango (*Mangifera indica* var. Kent and Brooks) peel powders useable as



healthy ingredients, *J. Food Meas. Char.*, 2024, **18**, 3665–3680.

142 Y. He, Y. Wang and S. Wang, Carbon dot and silver nanoparticle-based fluorescent probe for the determination of sulfite and bisulfite via inner-filter effect and competitive redox reactions, *Microchim. Acta*, 2023, **190**, 190.

143 S. Dluhošová, K. Bartáková, L. Vorlová, P. Navrátilová, O. Hanuš and E. Samková, Dairy Chain Safety in the Context of Antibiotic Residues—Current Status of Confirmatory Liquid Chromatography Methods: A Review, *Antibiotics*, 2024, **13**, 1038.

144 J. Wang, J. An, Z. Zhang, H. Zhu, X. Liang, S. Yang, K. Sheng, L. Chen, H. Lu and Y. Wang, High fluorescent nitrogen – doped carbon dots derived from *Sanghuangporus lonicericola* for detecting tetracyclines in aquaculture water and rat serum samples, *Microchem. J.*, 2023, **189**, 108517.

145 Y. Zheng, J. Hao, K. Arkin, Y. Bei, X. Ma, Q. Shang and W. Che, H<sub>2</sub>O<sub>2</sub>-assisted detection of melamine using fluorescent probe based on corn cob carbon dots-Ionic Liquid-Silver nanoparticles, *Food Chem.*, 2023, **403**, 134415.

146 A. Ghosh, K. Gautam, C. Gupta, C. Hazra, L. Das, N. Chakravorty, M. M. Mishra, A. Nain, S. Anbumani, C.-J. Lin, R. Sen, N. Dasgupta and S. Ranjan, Single-Step Low-Temperature Synthesis of Carbon Dots for Advanced Multiparametric Bioimaging Probe Applications, *ACS Appl. Bio Mater.*, 2024, **7**, 7895–7908.

147 J. Lin, X. Huang, E. Kou, W. Cai, H. Zhang, X. Zhang, Y. Liu, W. Li, Y. Zheng and B. Lei, Carbon dot based sensing platform for real-time imaging Cu<sup>2+</sup> distribution in plants and environment, *Biosens. Bioelectron.*, 2023, **219**, 114848.

148 Y. Li, J. Gao, X. Xu, Y. Wu, J. Zhuang, X. Zhang, H. Zhang, B. Lei, M. Zheng, Y. Liu and C. Hu, Carbon Dots as a Protective Agent Alleviating Abiotic Stress on Rice (*Oryza sativa* L.) through Promoting Nutrition Assimilation and the Defense System, *ACS Appl. Mater. Interfaces*, 2020, **12**, 33575–33585.

149 C.-Y. Wang, N. Ndraha, R.-S. Wu, H.-Y. Liu, S.-W. Lin, K.-M. Yang and H.-Y. Lin, An Overview of the Potential of Food-Based Carbon Dots for Biomedical Applications, *Int. J. Mol. Sci.*, 2023, **24**, 16579.

150 X. Pan, F. Fu, Z. Xie, W. Li, X. Yang, Y. Kang, S. Qu, Y. Zheng, Q. Li, H. Zhang, S. Song and B. Lei, Light-nutrition coupling effect of degradable fluorescent carbon dots on lettuce, *Environ. Sci.: Nano*, 2023, **10**, 539–551.

151 M. Gagana, B. R. R. Krushna, S. C. Sharma, B. Bommaalingaiah, B. Kar, S. Padmavathi, R. P. Ammal, R. Lalitha, R. Anitha, K. Manjunatha, S. Y. Wu and H. Nagabhushana, FRET enhanced CeO<sub>2</sub>:3Tb<sup>3+</sup> nanocomposites: a dual approach for photocatalytic dye degradation and agricultural safety, *Colloids Surf., A*, 2025, **720**, 137133.

152 S. A. Beker, L. S. Khudur, C. Krohn, I. Cole and A. S. Ball, Remediation of groundwater contaminated with dye using carbon dots technology: ecotoxicological and microbial community responses, *J. Environ. Manage.*, 2022, **319**, 115634.

153 X. Huang, S. Liu, X. Liu, X. Tan, S. Guo, M. Dai, Q. Chen, G. Chen and C. Feng, Doped carbon dots affect heavy metal speciation in mining soil: changes of dissimilated iron reduction processes and microbial communities, *Environ. Sci.: Nano*, 2024, **11**, 1724–1739.

154 L. Behera, A. K. D. Naik, B. B. Sahu and S. Mohapatra, Betaine-Modified Green Carbon Dot for Cr(VI) Sensing, In vivo Cr(VI) Imaging, and Growth Promotion in the Rice Plant, *ACS Appl. Bio Mater.*, 2024, **7**, 7624–7634.

155 J. Lin, W. Huang, H. Zhang, X. Zhang, Y. Liu, W. Li and B. Lei, A fluorescence probe based on blue luminescent carbon dots for sensing Fe<sup>3+</sup> in plants, *J. Mater. Chem. C*, 2024, **12**, 5480–5487.

156 Z. Yang, X. Yang, Q. Zhang, X. Zheng, Y. Zhang and C. Dong, Orange carbon dot nanomaterial as optical/visual sensing platforms for morin and a biomass booster for plant seedlings, *J. Environ. Chem. Eng.*, 2024, **12**, 114244.

157 N. A. Abdullah, H. E. Mahmoud, N. A. El-Nikhely, A. A. Hussein and L. K. El-Khordagui, Carbon dots labeled *Lactiplantibacillus plantarum*: a fluorescent multifunctional biocarrier for anticancer drug delivery, *Front. Bioeng. Biotechnol.*, 2023, **11**, 2023.

158 S. Sharma, T. M. Perring, S.-J. Jeon, H. Huang, W. Xu, E. Islamovic, B. Sharma, Y. M. Giraldo and J. P. Giraldo, Nanocarrier mediated delivery of insecticides into tarsi enhances stink bug mortality, *Nat. Commun.*, 2024, **15**, 9737.

159 P. K. Marvi, P. Das, A. Jafari, S. Hassan, H. Savoji, S. Srinivasan and A. R. Rajabzadeh, Multifunctional Carbon Dots In Situ Confined Hydrogel for Optical Communication, Drug Delivery, pH Sensing, Nanozymatic Activity, and UV Shielding Applications, *Adv. Healthcare Mater.*, 2025, **14**, 2403876.

160 B. A. Salha, A. Saravanan, M. Maruthapandi, I. Perelshtain and A. Gedanken, Plant-Derived Nitrogen-Doped Carbon Dots as an Effective Fertilizer for Enhanced Strawberry Growth and Yield, *ACS ES&T Eng.*, 2023, **3**, 1165–1175.

161 B. A. Salha, M. Maruthapandi, I. Perelshtain, J. H. T. Luong and A. Gedanken, Synergistic effects of nitrogen-doped carbon dots on pepper and lettuce growth via irrigation enhancement, *Diamond Relat. Mater.*, 2025, **152**, 111998.

162 T. He, X. Hao, Y. Chen, Z. Li, X. Zheng, M. Yang, Y. Wang, C. Gu, J. Ye and H. Wang, Promoting the growth of rice and reducing the accumulation of Cd in rice by pig bedding derived carbon dots (PBCDs) under Cd stress, *Environ. Sci.: Nano*, 2025, **12**, 863–878.

163 X. Guo, R. Yang, Y. Wang, S. Ni, C. Cheng and J. Sheng, Surface engineering and concentration-dependent emission activated flexible tunable fluorescence from lignin-based N-doped carbon dots, *Chem. Eng. J.*, 2024, **498**, 155146.

164 G. Tang, J. Wang, J. Xiao, Y. Liu, Y. Huang, Z. Zhou, X. Zhang, G. Hu, W. Yan and Y. Cao, Amphiphilic Cationic Carbon Dots for Efficient Delivery of Light-Dependent Herbicide, *Adv. Sci.*, 2024, **11**, 2406523.

165 Y. Liu, L. Zhang, H. Cai, X. Qu, J. Chang, G. I. N. Waterhouse and S. Lu, Biomass-derived carbon dots with pharmacological activity for biomedicine: recent advances and future perspectives, *Sci. Bull.*, 2024, **69**, 3127–3149.

166 C. Lei, Z. Ding, M. Tao, Y. Lu, L. Xu, B. Cheng, C. Wang and Z. Wang, Unraveling the distribution, metabolism, and catabolism of foliar sprayed carbon dots in maize and effect on soil environment, *J. Agric. Food Chem.*, 2024, **72**, 19710–19720.

167 J. Wang, M. Zhu, X. Zhu, Q. Zhang, Y. Yu, P. Zhao, M. Liu, R. Jin and Z. Tang, Divergent effects of biomass-derived carbon dots application and sweet potato planting on accumulations of soil microbial necromass carbon in Vertisol, *Appl. Soil Ecol.*, 2025, **210**, 106061.

168 Y. Chen, B. Lei, M. Zheng, H. Zhang, J. Zhuang and Y. Liu, A dual-emitting core–shell carbon dot–silica–phosphor composite for white light emission, *Nanoscale*, 2015, **7**, 20142–20148.

169 S. P. Chakradhar, B. R. R. Krushna, S. C. Sharma, S. Tripathi, C. Indhu, I. Jaiganesh, K. Manjunatha, S. Y. Wu, B. K. Das and H. Nagabhushana, Novel red-emitting CDs@LaCaAl<sub>3</sub>O<sub>7</sub>:Eu<sup>3+</sup> nanocomposites: a sustainable breakthrough for optical thermometry, indoor plant growth and intelligent security labels, *Mater. Chem. Phys.*, 2025, **335**, 130540.

